THERMAL CONDUCTIVITIES OF WOOD ASH, DIATOMITE AND THEIR COMPOSITE MIXTURES

BY

GAITHO, FRANCIS MAGIRI

PHYSICS DEPARTMENT

EGERTON UNIVERSITY

A thesis submitted in partial fulfilment for the degree of Master of Science in Physics at Egerton University.

EGERTON UNIVERSITY LIBRARY

1997

Eger241159

DECLARATION

This thesis is my original work and has not been presented for a degree in any other University.

Sign: _____ Date: 25/9/98

Name: GATHO FRANCIS MAGIRI

This thesis has been submitted with my approval as the University supervisor.

Sign: _____ Date: 25.09.98

Name: Prof. L. MUIA.

PHYSICS DEPARTMENT

EGERTON UNIVERSITY,

P.O. BOX 536, NJORO.

COPYRIGHT ©

No part of this thesis may be produced, stored in any retrieval system or transmitted in any form or means; electronics, mechanical, photocopy, recording or otherwise without prior written permission of the author or Egerton University on that behalf.

ABSTRACT

The transient hot-strip (THS) method was used to investigate the thermal conductivities of samples in their consolidated or moulded forms. Two different porous materials, i.e., wood ash and diatomite (F and Bu types), as well as their composite mixtures were used in this investigation. The samples were grouped in various particle sizes, their porosities determined, and their physical as well as chemical characteristics discussed. Thermal conductivity variations of the samples, with the factors; particle size, porosity, moisture content, composition of the mixtures and temperature were investigated.

F diatomite samples in general displayed high thermal conductivity values of up to 8.92 x 10^{-2} W m^{-1} K^{-1} at room temperature and 0 % moisture content. There were low values for wood ash; 2.25 x 10^{-2} W m^{-1} K^{-1}, while Bu diatomite displayed moderate values for the same conditions. In comparison with the pure samples, the composite mixtures of wood ash, Bu and F diatomite showed very low values. These ranged from 1.26 x 10^{-3} W m^{-1} K^{-1}, for the 75 % wood ash/ 25 % Bu composite, to 6.796 x 10^{-2} W m^{-1} K^{-1} for the 50 % F/ 20 % wood ash/ 30 % Bu composite mixture. A comparison of these results obtained using the THS method, and those obtained in theoretical models of determination of thermal conductivities of porous media shows satisfactory agreement. These materials could be used as thermal insulators and fluid adsorbents mainly due to there well defined porosities, wide pore size distribution and ability to retain moisture. The interlock between individual particles in the composites provides a possibility of the composites to be used as fillers and binders.

ACKNOWLEDGEMENTS

I am very grateful to my sister, Sr. Jude, for her support both financially and materially. It is through this support that I have been able to carry out the entire research and further my studies.

My thanks to my supervisor Prof. Muia for his helpful suggestions, critical comments, encouragement and reading of this thesis. Through that trying time of my research, he tirelessly guided me into the right path.

Many thanks to Robert Kamau Kinyanjui and colleagues in the Physics department. Through their wise counsel and encouragement, I was able to go over the difficulties that arose during research and writing of this thesis.

For the technical assistance accorded to me, my thanks go to the staff of engineering and Chemistry departments in Egerton University. Appreciations to the technicians of Physics department for the support they gave during preparation and setting of research facilities.

To all those who in one way or another, directly or indirectly and without my consent, contributed positively towards success of this work, thank you very much. In particular, I am indebted to my MSc. colleagues, friends, mum, dad, brothers and sisters for the time they availed during their valuable comments.

DEDICATION

To my forbearing wife Lilian, daughter Gathoni and Sr. Jude Njeri, without whose encouragement, patience and support my academic goals would not be attained.

SYMBOLS USED

α	Temperature coefficient of resistivity of the Hot- strip,
β	Euler's constant,
Δx	Thickness of the substance used,
$f(\gamma)$	Solution to heat problem,
$f(\gamma)$	Solution to heat problem,
$f(\gamma)$	Solution to heat problem,
κ	Thermal diffusivity,
Λ	Thermal conductivity,
Λ_s	Porous system thermal conductivity,
Λ_{eff}	Effective thermal conductivity,
Λ_{TD}	Theoretically dense thermal conductivity,
Λ_j	Thermal conductivity in the j^{th} direction,
ψ	Phase angle,
ρ	Porosity,
σ	Thermal conductance,
σ_{eff}	Effective thermal conductance,
θ	Characteristic time,
$\frac{\partial T}{\partial x_j}$	Temperature gradient in the j^{th} direction,
$\Delta T = T_1 - T_2$	Temperature difference between two points of temperatures T_1 and T_2,

2ν	Thickness of the Hot- strip,
2d	Width of the Hot- strip,
2h	Length of the Hot- strip,
A	Area of cross section of material,
Bu diatomite,	Diatomite type obtained from Soysambu mines in Gilgil
C	Specific heat,
d	Thickness or diameter of the heat source (Hot- strip),
D	Density of material
D_b	Bulk density,
D_p	Particle density,
d_ω	Density of water,
Ei	Exponential integral,
erf	Error function,
F diatomite,	Diatomite type obtained from Kariandusi mines at Giligil in the Rift valley of Kenya
I	Instantaneous current at time t,
I_o	Current across the heating element before transient heating,
J	Current density at steady state conditions,
M_ω	Weight of water saturated sample,
M_s	Mass of solid oven dried particles,
N	Number of solid particles in a total volume V of sample,
P_o	Power out put per unit length of the Hot-strip,

Q	Quantity of heat supplied or removed,
R	Varying resistance of the Hot- strip (heat source),
R_1	Current limiting resistance,
r_1, r_2	Radii at distances 1, 2 from the heat source,
R_2	Balancing resistance,
R_L	Resistance as a result of narrowing lines of heat flow in an elementary cell of the sample,
R_o	Initial resistance of the Hot- strip,
R_{sp}	Resistance of microroughness at the place of contact,
t	Transient time of heating,
t_c	Time correction factor depending on the heating probe and thermal properties of the sample,
$T_o \sin\omega t$	Sinusoidal variation of temperature at one end of sample at steady state conditions,
V	Instantaneous voltage at time t,
V_1	Volume of solid phase of an elementary cell of the sample,
V_2	Volume of the gaseous phase in a unit cell of the sample,
V_a	Volume of water absorbed by sample,
V_b	Bulk volume,
V_o	Voltage across heating element before transient heating,
W	Percentage moisture (water) content,
W_ω	Weight of pycnometer with water,

W_a	Weight of air in pycnometer,
WA	Wood ash samples
W_s	Weight of sample in pycnometer,
$W_{s\omega}$	Weight of pycnometer with sample and air.

TABLE OF CONTENTS

PAGE

DECLARATION ii

COPYRIGHT iii

ABSTRACT iv

ACKNOWLEDGEMENTS v

DEDICATION vi

CHAPTER 1 1

1.0 INTRODUCTION AND OBJECTIVES 1

1.1 Introduction 1

1.2 Objectives 5

CHAPTER 2 6

2.0 LITERATURE REVIEW 6

2.1 General properties of Diatomite 6

2.2 General properties of Wood ash 9

2.3 Properties of porous materials 11

2.4 Thermal conductivity measurements 14

2.4.1 Thermal insulators 16

2.4.2 Composites 18

CHAPTER 3 20

3.0 THEORY AND GENERAL DESCRIPTIONS 20

3.0.1 Basic definitions 20

3.1 Theory of heat transfer 21
3.1.1 Modes of heat transfer 22

3.2 Methods of measurement of thermal conductivity 23
3.2.1 Steady state (static) methods. 26
3.2.2 Non-steady (Dynamic) state methods 29
3.2.3 The Transient-Hot Strip (THS) Method. 39

3.3 Factors affecting thermal conductivity of porous systems 43

3.4 Theoretical models for prediction of thermal conductivity 49
3.4.1 Wimmer's model 49
3.4.2 The model of Luikov et al 51

CHAPTER 4 54

4.0 EXPERIMENTAL TECHNIQUES 54

4.1 Measurement of particle size 54

4.2 Determination of density and porosity 56
4.2.1 Bulk density 56
4.2.2 Measurement of particle density of unconsolidated sample 57

4.3 Preparation of sample composites 58

4.4 Slab preparation (Consolidated sample) 60

4.5 Determination of porosity of consolidated sample 61

4.6 Moisture content 62

4.7 Measurement of temperature 63

4.8 Method of measurement of thermal conductivity 63
4.8.1 Experimental method 65
4.8.2 Experimental circuit 66

CHAPTER 5 68

5.0 RESULTS AND DISCUSSION 68

5.1 Physical and mineralogical analysis 68

5.2 Composition of composite mixtures 71

5.3 Particle size distribution analysis 78
5.3.1 Thermal conductivity and particle size 81

5.4 Thermal conductivity and porosity 84

5.5 Variation of thermal conductivity with moisture content 86

5.6 Variation of thermal conductivity with temperature 89

CHAPTER 6 92

6.0 CONCLUSIONS AND RECOMMENDATIONS 92

6.1 Conclusions 92

6.2 Recommendations 93

REFERENCES 95

APPENDIX I 100

APPENDIX II 101

APPENDIX III 102

APPENDIX IV 103

LIST OF FIGURES

FIGURE: PAGE:

2.1 Pore and grain arrangement of a material 12

2.2 A comparison of variation of thermal conductivities with porosities of consolidated sandstone and unconsolidated sand, ... 15

3.1 Measurement of thermal conductivity of a piece of wood 24

3.2 Principle of steady-state longitudinal heat flow method for measurement of thermal conductivity, ... 27

3.3 Principle of steady-state radial heat flow method of measurement of thermal conductivity. 28

3.4 Variation of thermal conductivity per unit of water added in to silty loam soil 44

3.5 General variation of thermal conductivity with porosity for most powders. 45

3.6 Variation of effective thermal conductivity of copper powder samples with porosity 46

3.7 Variation of effective thermal conductivity of copper powder with particle size 47

3.8 Variation of thermal conductivity of different materials with temperature 48

4.1 Plastic slab moulding box 60

4.2 Typical experimental arrangement of theTHS method 63

4.3 Circuit diagram for measurement of thermal conductivity 66

5.1 Variation of thermal conductivity with percentage composition by mass of composite mixtures comprising 3 samples. 75

5.2 Variation of thermal conductivity with percentage composition by mass of composite mixtures comprising 2 samples. 76

5.3 Percentage by weight of particle size distributions for wood ash, Fand Bu diatomite 80

5.4 Variation of thermal conductivity with particle size for wood ash, F and Bu diatomite 83

5.5 Variation of thermal conductivity with porosity for wood ash, Bu and F diatomite 85

5.6 Variation of thermal conductivity with moisture content for wood ash, Bu and F diatomite 87

5.7 Variation of thermal conductivity with temperature for samples of wood ash, Bu and F diatomite and their composites 91

LIST OF TABLES

TABLE: PAGE:

1 Composite mixture of only two samples 58
2 Ccomposite mixtures of B, C samples with A constant 59
3 Composite mixtures of A and C with b constant 59
4 Composite mixture of A and B with C constant 60
5. Wood ash mineralogical composition 68
6. Diatomite mineralogical composition 68
7 Physical description of wood ash,F and Bu diatomite 69
8. Thermal conductivities of composite mixtures of wood ash, F and Bu diatomite, (wood ash constant) 71
9. Thermal conductivities of composite mixtures of wood ash, Fand Bu diatomite, (F diatomite constant 71
10. Thermal conductivities of composite mixtures of wood ash, F and Bu diatomite, (Bu diatomite constant 72
11. Thermal conductivities of composite mixtures of F and Bu diatomite 73
12. Thermal conductivities of WA and F diatomite composite mixtures 73
13. Thermal conductivities of wood ash and Bu composite mixtures 74
14. Sample particle size distribution 78
15. Percentage by dry weight of wood ash, F and Bu diatomite retained by respective sieve sizes . 78
16. The adjustments to be made to a mass of sample when it is necessary to increase or decrease its moisture content to a required value 100
17. Value of $f(\gamma)$ for different values of time (t), at constant characteristic times (θ), in the range $0.1 \leq \theta \geq 1.0$ 103

CHAPTER 1

1.0 INTRODUCTION AND OBJECTIVES

1.1 Introduction

In the recent years there has been an increasing awareness that man is rapidly depleting the available energy resources. This awareness has not only initiated efforts to find new energy sources, but has also inspired attempts to reduce the general energy consumption both industrially and domestically. Most of the energy we use and most of the energy we save is in form of heat. In cold weather, for example, we are interested in transferring heat from furnaces, wood and charcoal stoves etc., into our rooms to provide warmth. At the same time we are interested in preventing this transfer of heat from the interior of the building to the outside and vice versa during hot weather. This prevention is done by use of materials which best prevent the heat transfer- thermal insulators.

There have been publicity drives to reduce the domestic consumption especially that of wood and related fuels. As a result this save energy campaign and a general increase of interest in technical subjects and growth of technology , the number of those who require some knowledge of heat and the flow of heat has risen, consequently, application and understanding of physical properties of porous systems have increased. These properties which are interrelated determine the areas which the systems are most applicable.

The greatest interest in porous systems is due to the fact that they have found wide application in a number of industrial branches, for example, in areas where an understanding of

the basic physics of thermal characteristics, that enhance or resist application, of these systems is required.

Little quantitative information is known about some porous wastes like wood ash and saw dust ash, yet these wastes may prove very useful if well explored. For example, traditionally wood ash is smeared on walls of houses to prevent or minimise heat transfer, possibly due to its low thermal conductivity. It may also be used as a filler in plaster (Gerald et al, 1984). In some regions of the world, wood ash is mixed in small proportions with cattle or goat dung, then made into cakes and dried. Wood ash is used in this case to prolong the burning process. Ash may also find its use as a colouring agent. The potential of wood ash as a thermal insulator is exploited by maize roasters who cover their open fire with it to control the rate of fuel burning in addition to minimising heat loss (Aduda, 1987).

Diatomite on the other hand is only found in specific locations, where there is infusorial or diatomaceous earth. It is a siliceous sediment made up more or less entirely of skeletal remains of microscopic plants called diatoms. The structure, colour and density are location specific. Diatomite is of great economic importance in industrial application. For example it is processed and used as a thermal insulator, a filter aid, fluids absorbent, a ceramic material and in the explosive industry etc., (African diatomite Industries, Gilgil 1996). Much has been done on diatomite and related materials. More often these materials have been chosen for use, but certain criteria such as strength, durability, weather resistance, thermal resistance and stress, flammability and cost conflict with each other (Cornish, 1987). A link therefore appears to be missing interrelating these criteria, material property and characteristics with their various applications.

A knowledge of thermal properties of porous systems i.e., thermal conductivity, diffusivity, specific heat, and thermal stress is essential in the design of thermal insulating materials and refractories. Diatomite is also important in the explosives industry, nuclear reactors and in oil explorations (Touloukian, 1970).

The focus of this work will be on measurement of thermal conductivities of wood ash and diatomite against various physical factors. The choice of wood ash and diatomite as study materials was based on the following,

(i) availability,

(ii) both are porous materials that can be easily handled (they are inert),

(iii) in their finest particle state both can be moulded into slabs.

By definition, thermal conductivity is the physical property denoting the ease with which a particular substance can accomplish energy transmission by molecular motion (Chapman, 1990). Physically, it also represents the amount of heat flow through unit thickness of the material when the temperature difference across the thickness is unity (Arora, 1989). This can be expressed as;

$$\Lambda = \frac{[Q][\Delta\chi]}{[A][\Delta T]} \qquad (1.0)$$

where, Λ is thermal conductivity,

Q is quantity of heat,

$\Delta\chi$ is thickness of the substance,

A is cross-sectional area of the material,

ΔT is temperature difference across the thickness.

For a given thickness of material exposed to a given temperature difference, the rate of heat flow per unit area is directly proportional to the conductivity of the material (Sybil, 1981).

In derivation of equation (1.0), the solid is assumed to be homogeneous and of such a material that, when a point within it is heated, the heat spreads equally in all directions. According to Carslaw and Jaeger (1959), such a material is said to be isotropic as opposed to anisotropic solids in which certain directions are more favourable for the conduction of heat than others. We also have heterogeneous solids in which the conduction conditions vary from point to point as well as in direction. In solids, heat is conducted by both lattice vibrations and transport by free electrons. Non-metallic materials have no free electrons, hence have low thermal conductivities.

In general thermal conductivity is not constant for the material but varies with temperature. For metals and other crystalline materials, conductivity decreases with increasing temperature; for gases and other amorphous materials, conductivity increases with temperature (Sybil, 1981). It is well known that thermal conductivity and thermal diffusivity of porous materials extensively depend on the structure, density, porosity, temperature and heat capacity. These properties also exhibit a strong dependence upon temperature and pressure. Development of effective solutions to the problems of thermal insulation especially using porous composites is perhaps one of the most challenging applications of the knowledge of thermal conductivity and thermal diffusivity.

1.2 Objectives

The objectives of this study are to;

(i) investigate experimentally the variation of thermal conductivity of wood ash and diatomite as a function of parameters like porosity, concentration of composite mixtures, temperature and particle size distribution using the transient hot-strip (THS) method.

(ii) study the mineralogical and physical properties of wood ash and diatomite,

(iii) explain the differences in thermal conductivity between wood ash and diatomite,

(iv) study the effectiveness of diatomite/ wood ash composites in various proportions as binders and thermal insulators.

(v) compare experimental and theoretical values so as to obtain a theoretical model that could be used to calculate thermal conductivity of porous systems.

CHAPTER 2

2.0 LITERATURE REVIEW

2.1 General properties of Diatomite

Natural diatomite comprises of opaline silica skeletons of various species of diatoms that flourished in marine or fresh water environments hundreds of years ago. Information from the African Diatomite Industries in Gilgil Kenya, (1996), reveal that diatomite is location specific. The structure, the colour , density depend on the mine from which diatomite is obtained.

Analysis of diatomite sediments from a Paleolake in central Mexico has been done by Miranda et al, (1994) using proton induced X-ray emission (PIXE), X-ray tomography and X-ray diffraction. In their finding , three different kinds of layers were seen, related to their colours: dark, white and grey. The composition of the layers was fairly uniform. The dark zone was enriched in Al, K, Ca, Ti, Mn and Fe. This dark layer may be associated with eruptions of the Malitzin volcano. The white zone was found to contain diatomite of high purity, with traces of K, Ca and Fe, while the grey zone suggested that there was a clay contamination of diatomite. Using X-ray diffraction, it was concluded that the white and the grey phases were highly amorphous, with a small component of cristobalite, as expected from the diatom sediment diagenesis, while the dark layer contained large amounts of anorthite and orthoclase, supporting the volcanic origin in this layer (Miranda et al, 1994).

In its preparation for industrial use as a filter aid, diatomite is heated to temperatures about 1000 °C. At these temperatures fusion takes place and capillaries are destroyed. This heating process (calcination) `burns out' some of the finest tertiary silica structure and helps sinter fines together . In flux calcination, heating is accompanied by addition of a flux such as sodium

chloride or soda ash. This process also helps to improve the colour of diatomite. Calcination modifies the flow rate of filter aids (Hey, 1969).

A good filter aid must posses several characteristics. These include, the ability to form a very porous cake, a low surface area, correct particle size distribution and non-uniform sizing and availability in a number of grades. Performance of diatomite and other mineral filter aids is measured by the clarity of the filtrate, the rate of flow of the liquid through the filter bed and the length of the filter cycle. Diatomite as a filter aid is used in food products such as beer, wine, fruit and vegetable juice and spirits. It is also used in metallurgical processes, petroleum refining and processing, drug and pharmaceutical manufacture (African Diatomite Industries, 1996). The most widely used of all mineral filter aids is diatomite (diatomaceous earth) due to its low bulk density. It is essentially inert, non-compressible, highly porous and permeable.

Mineral sorbents are employed in the purification of edible oils and fats by selective absorption and also in absorption of insecticides, herbicides and other agricultural chemicals. These minerals are highly absorbent and adsorbent in their natural or modified form. A high surface area is the leading factor in the absorptive capacity of these minerals. For the same material we can obtain both high and low surface areas depending on the application.

Studies of sorption of benzene by diatomite were made by Odhiambo, (1969). He found that the surface area of diatomite decreases with increase in temperature in steps from 300 °C to 400 °C, 700 °C and then to 1000 °C. By gravimetric methods (BET- Brunauer, Emmett, Teller), surface area was found to be 30.1 m^2g^{-1}, which when treated with warm 3N hydrochloric acid increases by 20 %. The same study found that when pressure on diatomite is decreased, the pores emptied when the relative pressure fell below a certain value. The volume of the emptied pores

was obtained from the amount of the gas desorbed from the capillary condensed liquid with allowance being made for the remaining absorbed film.

Diatomite ore contains less than 10 % of metallic oxide impurities. These oxides may either be located in certain pores, blocking the capillaries, or be thinly distributed over the diatomite surface. Washing the diatomite with acid (acid treating) removes these oxides. Acid treated diatomite is nearly 100 % porous hydrous silica (Odhiambo, 1969). Sorption of benzene by acid treated diatomite has been studied in order to explicate the effect of the presence of oxides on the porous structure of diatomite.

High gradient magnetic separation (HGMS) tests have been carried out to remove magnetic impurities from a slurry of diatomite from different deposites in Bulgeria (Videnov et al, 1993). It was found that at magnetic fields greater than 0.5 T, magnetic separation achieves very high removal of magnetic impurities. The experimental investigations show that the recovery and the grade of the product depends upon the source of the raw material.

Studies have also been made on diatomite as a filler. According to studies of filler and coatings of siliceous minerals ,they are generally inert in most applications since their pH values lie in the range 6-10 and refractive index between 1.4 and 1.7 (Severinghaus, 1983). Small amounts of impurities do not adversely affect the utility of the products for filler uses, although they may affect colour or brightness which is important in some applications. Impurities may also affect expansion characteristics and some applications of silica and ceramic that require high purity for colour. Fillers essentially control gloss and sheen, modify solvent release and improve sanding resistance (Sybil, 1981).

In a study on thermal-conversion of filled polymer composites of Aminoplast on the basis of diatomite it was found that thermal treatment led to an increase of the rate and depth of curing due to the catalytic action of the filler. These polymer compositions are capable of injection moulding and yield plastic materials with good dielectric properties (Mgeladze et al, 1991).

Other applications of diatomite include (Severinghaus, 1983);

(i) roofing, where it can supply weathering resistance and strength,

(ii) insecticides, where it is used to provide chemical inertness and control dilution for even distribution,

(iii) abrasives, where it supplies controlled particle size, friability and various hardness.

(iv) paper (as a filler), where it can supply 'tooth' pitch control, porosity and cohesion,

(v) insulation for concrete, plastic, acoustic products and refractory building brick. Here diatomite supplies light density, thermal stability, low thermal conductivity and inertness.

This last application is the main focus of this work.

2.2 General properties of Wood ash

Little work has been done about wood ash even though it occurs in abundance. Wood ash is a residual material produced during the process of biomass burning of energy. It may consist of minerals like Silica, Alumina , Iron oxide etc. Wood ash is a potential thermal insulator, (Aduda, 1987) as well as a refractory or ceramic material. Spreading this material on the land is used as means of disposal.

Wood ash contains carbonates which react to raise soil pH (Erich and Ohno, 1992) and its regulation is based on ash calcium carbonate equivalent (CCE), the procedure suggested by the

Association of Official Analytical Chemists (AOAC) for the determination of the CCE in wood ash samples. This procedure involves heating a weighted amount of sample with Hydrochloric acid (HCl) and then back-titration of the remaining acid with Sodium hydroxide (NaOH). Unlike agricultural lime stones, which are largely carbonates, some wood ash samples contain significant amounts of contaminants such as Alumino-silicate clays which may consume acidity when heated with HCl. Significant consumption of acidity by Alumino-silicates during CCE analysis would cause the determination of artificially high CCE value, as these Alumino-silicates would not be expected to neutralise acidity under field conditions. In their study Erich and Ohno, (1992) investigated whether the AOAC method of CCE determination resulted in reproducible, accurate CCE values when applied to wood ash samples with various amounts of Alumino-silicate contaminants. The accuracy of the method was calculated by comparing the CCE values with those obtained from a soil incubation method. Time of heating had little effect on the CCE value obtained. The back titration step was reproduced from operator-to-operator despite the formation of a white precipitate before the end point. The CCE values obtained from the titrimetric method were similar to those obtained from a soil incubation method.

Colour is one of the more obvious characteristics and one that is more frequently used to describe materials. The colour of wood ash depends on the firing conditions and the type of wood used. Colour is a composite of the colours of the components comprising wood ash. The effect of these components on the colour of the composite is roughly proportional to their total surface which is equal to their specific surface times their volume percentage in the sample, (Helmut, 1968).

The most outstanding components are iron hydroxide and silica. Iron oxide may be red, rust-brown or yellow, depending on the degree of hydration. Reduced iron is blue-green. Silica is mostly white or greyish. In comparison with wood ash, some clays are grey, white or red. The colour of clays is largely determined by the type and the amount of iron coatings. Wet and moist samples of wood ash look darker than dry samples. The reason for this is that the reflective properties of the solid components and the air are very different and that the light that falls on a dry sample is highly reflected. The reflective properties of water and porous granular samples are sufficiently similar that light penetrates the sample and much of this light is absorbed. As opposed to light materials, dark materials tend to be warmer in warm atmosphere thus absorb energy. This effect may cause the material to undergo thermal stress leading to cracking and splitting of the particles.

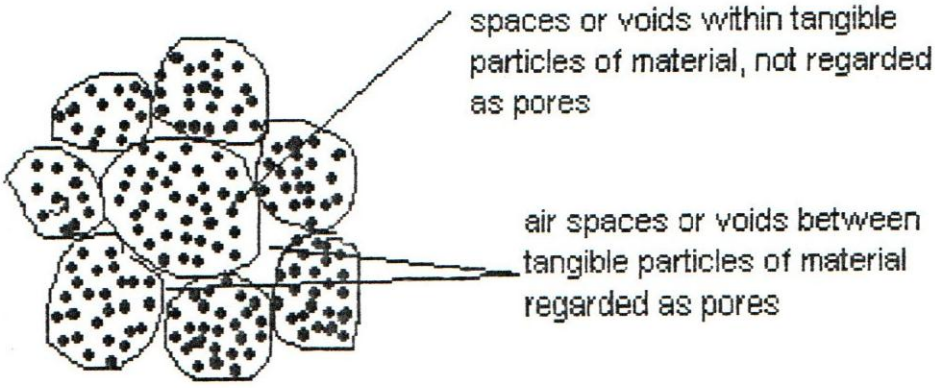
Wood ash is a potential thermal insulator, for example it is typically mixed with cow dung then smeared on walls of houses to act as a plaster and a thermal insulator. This may be due to its low ability to conduct heat and its appearance (colour).

2.3 Properties of porous materials.

There are many different ways in which materials can be classified. There are already quite a number of ways which are related to a particular performance which materials are capable of, such as thermal insulation, acoustic insulation, absorption of water. Many solid systems of practical importance are porous, i.e., the solid matrix is interspaced by voids, ranging in size from molecular dimension upwards. The pore structure of a material can be described in terms of its porosity, pore size distribution and specific surface.

Materials such as diatomite and other minerals occur naturally in a porous condition (severinghaus, 1983), while in others, the pore structure is produced intentionally during manufacture in order to achieve certain desired properties. However, the actual structure and to some extent the physical behaviour of a material is dictated by the arrangement of the pores.

Fig. 2.1 Pore and grain arrangement of a material



For example, the exploitability of reservoir rocks is related to the permeability, which in turn is strongly influenced by dimensions, shape and connectivity of the pores (Helmut, 1968). The pore structure of natural and artificial building materials influences their mechanical resistance and field performance.

It has been shown that many useful properties of materials such as mechanical strength, permeability to fluids, thermal transmission and acoustic transmission are directly influenced by the size, extent and arrangement of pores (Lyall, 1992). Quantitative relationships that would be used to express these dependences are however not reliable. On one hand, theoretical treatments rely heavily on the use of simplified models to reduce the geometrical complexity of the pore

structure to a more tractable form, while on the other hand, empirical relationships, though abundant, lack generality because of variability of most porous systems. Therefore it is difficult to draw valid general conclusions because of a lack of reliable and strictly comparable data since these materials have wide range of applications.

Generally porous materials can be regarded as either consolidated or unconsolidated. In consolidated systems, the solid phase forms a rigid spongy structure in which it is impossible to isolate individual particles, pores are closed or connected to each other by one or more paths (Woodside and Messmer, 1956). In an unconsolidated corpuscular system, pores are formed by the spaces between discrete particles, the shape and dimensions of pores depend on those of the constituent particles and their mutual arrangement, i.e. the larger the particles and the lesser the compaction, the greater the pore dimension.

Many porous systems are used as acoustic and thermal insulators. Acoustic absorption depends essentially upon the wavelength of the incident sound and the thickness of material used (Touloukian, 1970). The influence of the pore structure is usually evaluated on the basis of the density of the material itself. For artificial porous materials the size of the cells and their connectivity, can be controlled during the manufacturing process. The cell structure influences the efficiency and the life of the insulator. Thermal absorption depends on the intensity and distance of the heat source, as well as the influence of the pore structure. In the case of uniform structure, small cells give a low value of thermal conductivity (Touloukian, 1970).

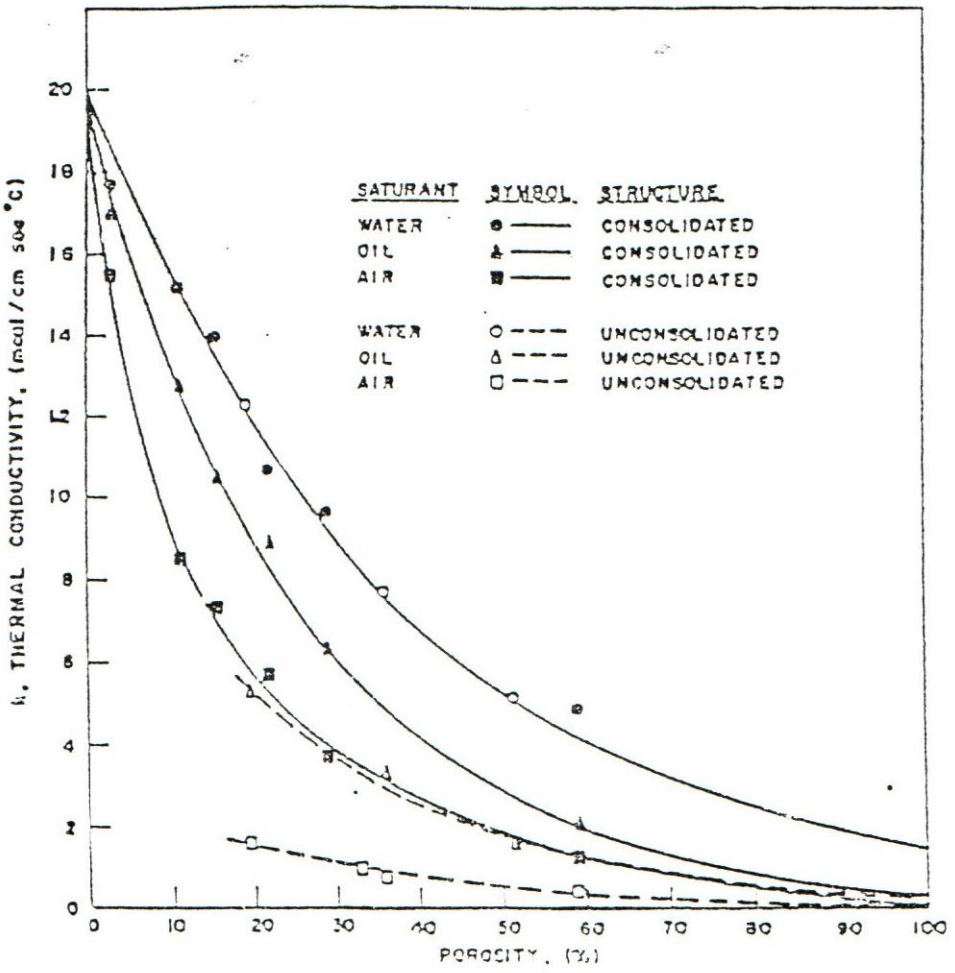
2.4 Thermal conductivity measurements

Thermal conductivity of fired refractory clays: Kaolin, fire clay, Siaya clay, Kisii soap stone have been measured by Kimani, (1989). He used the transient hot wire (THW) method of comparison. Thermal conductivity of the clays in dry air at atmospheric pressure was determined at different porosity percentages as a function of temperature from room temperature to about 800 °C. The effects of particle size distribution, chemical composition, grain structure and firing shrinkage were also investigated. The study established that thermal conductivity decreased with increase in percentage porosity, while it increased with increase in moisture content and temperature.

Similarly the THW method was used to determine thermal conductivity of two types of unfired clays: black and red from the central province of Kenya, (Kinyanjui, 1995). Some general trends of variation of thermal conductivity values against, temperature moisture content, porosity and particle size were obtained and compared to those obtained by Kimani, (1989). It was found that thermal conductivity also depends on organic matter in the samples (Kinyanjui, 1995).

Effective thermal conductivity of porous media e.g., consolidated rocks with porosity ranging from 3 % to 59 % have been determined (Woodside and Messmer, 1956), as shown in Fig. 2.2 below. The method used was based on the transient heating effect resulting from a line heat source. The study showed the variation of saturating fluid and the pressure of air filling the pore space and overburden pressure. On comparison with results of unconsolidated sands, all samples except one exhibited a lower thermal conductivity when saturated with a gas at atmospheric pressure than when saturated with liquid of the same conductivity as the gas.

Fig. 2.2 A comparison of variation of thermal conductivities with porosities of consolidated sandstone and unconsolidated sand, (Woodside and Messmer, 1956)



Considering both radiation and conduction of heat, Helte, (1993) studied the effective thermal conductivity (Λ_{eff}) of porous media. Expressions for Λ_{eff} of a solid containing dispersed, equisized, disconnected spherical pores were derived within an extended effective medium theory. With radiation present, the results agreed well with exact experimental results for an fcc lattice of spheres. The effective medium approach was also used to calculate the transverse effective thermal conductivity for a solid containing aligned, infinitely long, equisized, disconnected cylindrical pores. Without radiation, the result was in excellent agreement with exact results for a hexagonal array of cylinders. In the direction parallel to the cylinder axes, Λ_{eff} was found exactly.

For powdered systems and solid porous materials, the processes of heat transfer have many similarities. Reported data on thermal conductivity of pure materials (crystals and amorphous solid bodies, metals, gases, fluids) are numerous. Thermal conductivities of porous materials comprising pure substances depend on the properties and volumetric proportions of the pure materials they comprise, (Luikov et al, 1966).

2.4.1 Thermal insulators

Insulating materials are used where one wishes to minimise the flow of heat between an enclosure and its surroundings. Low temperature insulations are found where the enclosure is at a lower temperature than ambient temperature and when one wishes to prevent the enclosure from gaining heat. High temperature insulations are used in the reverse case when one wishes to prevent the enclosure from loosing heat.

Cork, mineral wool, glass wool etc., are examples of low temperature insulations. Asbestos, diatomaceous earth, magnesia and most refractories (materials used in instances desired

to withstand high temperatures without physical deterioration), are examples of high temperature insulations, (Chapman, 1989). Categories of insulating materials include;

(i) loose fill or granular insulation, made from expanded materials such as vermiculite ,diatomite or from ground vegetable matter such as granulated cork,

(ii) slab insulation which is made from cork, shredded wood, cement, mineral wool with binder, vermiculite, diatomite and asphalt, foamed plastic, cellular hard rubber or from expanded clays. The insulative value of these materials lies in the fact that the basic material is a poor conductor of heat and that the finished product is very porous.

(iii) reflective insulations, composed of metallic or other special surfaces with or without some type of backing. They rely on their surface characteristics, thickness of air spaces and temperature difference for their insulating ability.

The effective thermal conductivity of loose particulate insulation systems, in the temperature range from 273 K - 900 K have been compared to those predicted from three different models (Aduda, 1996). The results showed that the measured values of thermal conductivities of brick powder, white pottery clay, red ant-hill soil swamp clay, black pottery clay and vermiculite , increase with temperature.

For slab insulations Jaganmohan and Sukhatme, (1968), determined thermal conductivity and heat capacity simultaneously. The technique was to subject the insulation specimen initially at a uniform temperature, to a heat flux on one of its faces, the other being maintained at its initial value. The two properties, heat capacity and thermal conductivity, were determined by marching the experimental temperature-time history with that predicted theoretically in a least square error sense. A large number of tests have been conducted on several types of insulating materials such

as cork-board glass wool and polystyrene foam (Jaganmohan and sukhatme, 1968). The values obtained with transient method have been compared with those obtained by a steady-state technique. Good agreement was obtained.

Miller and Kotlar, (1993), described an experimental technique for the simultaneous measurement of thermal diffusivity and conductivity of small specimens of insulating material. Experimental conditions closely approached the mathematical idealisation of a one-dimensional, infinite two component composite solid whose planar interface was subjected to a step function heat flux. The heat flux was generated by resistive heating of a thin metallic foil. This technique permitted specimens with volumes two orders of magnitude smaller than those previously used in studies based on the same idealisation.

2.4.2 Composites

A composite material is one composed of two or more distinct phases, one of which is a matrix surrounding the fibres or particles of the other, there being some form of bonding at the interface between them. A composite has the desired properties that are not exhibited by either of the material on its own, (Pascoe, 1978). For example, a single phase material may have high strength and low density, but because it is brittle or not formable in large sections, it cannot be used on its own, hence mixed with another that not brittle or formable in large sections.

Garret and Rosenberg, (1974), investigated the various factors operative in determining the thermal conductivity of composite materials of non-metallic powders set in epoxy-resin matrix. The results which indicated that the thermal conductivity at low temperatures showed quite different features from room temperature behaviour, could be interpreted in the light of

current theoretical work. For temperatures below 20 K, the conventional Searl`s bar was used for the experiment. The specimens were cut to a length of about 25 mm and mounted with one end in thermal contact with a hydrogen or helium bath of a cryostat, which acted as a heat sink. The other end of the specimen was heated electrically and the temperature gradient along the rod was measured by using an iron/ chromel thermocouple attached to two copper contacts which were set into the specimen about 10 mm apart. Due to the low thermal conductivity of the specimen, this technique was inaccurate at 77 K and above because radiation losses were too high. To reduce those losses thermal conductivity in the temperature range 77 K to 300 K was measured with the specimen in the form of a miniature Lee's disc - about 5 mm in diameter and 2 mm thick. This was sandwiched between plates in which different copper/ constantan thermocouple contacts were embedded to determine the temperature gradient across the specimen.

The results obtained by Garret and Rosenberg (1974), revealed that the thermal conductivity of epoxy and epoxy filler composites increased monotonically with temperature. Temperature dependence of conductivity of these composites above 20 K was similar to that of the unfilled epoxy. The value at a given temperature was, in general, dependent on the volume concentration of the filler and on its thermal conductivity. In all the samples the composite conductivity above 20 K was higher than that of the unfilled resin and it increased with increasing filler concentration. Below 20 K, an increasing filler concentration decreased the conductivity. At very low temperatures there was pronounced particle size effect. Thus a reduction in particle size decreased thermal conductivity to very low values.

CHAPTER 3

3.0 THEORY AND GENERAL DESCRIPTIONS

3.0.1 Basic definitions

Heat conduction is interpreted either as molecular interchange of kinetic energy or electron drift (Carslaw and Jaegar, 1959). In the former, as the molecules of the material are heated they are set into motion and they in turn by elastic impact set their neighbouring molecules into motion, throughout the thickness of the material, in the latter, heat conduction is associated primarily with the mobility of free electrons.

As stated in chapter 1 of this thesis, thermal conductivity (Arora, 1989), is the proportionality factor in the conduction equation (Mohsenin, 1980);

$$Q = -\Lambda A[\frac{\Delta T}{\Delta X}] \qquad (3.0)$$

The negative sign simply show that the temperature gradient here decreases with time

$$[\Lambda] = \frac{[Q][\Delta X]}{[A][\Delta T]} \qquad (3.0.1)$$

Units of Λ are derived as;

$$\frac{[Js^{-1}][m]}{[m^2][K]}$$

$$= W\ m^{-1}\ K^{-1}\ \text{(Watts per meter per Kelvin)}$$

$1\ W\ m^{-1}\ K^{-1} = .86\ K\ Cal\ hr^{-1}\ m^{-1}\ {}^{o}C^{-1}$ (Kilocalories per hour per meter per degree Celsius) also,

$1\ W\ m^{-1}\ K^{-1} = .578\ Btu\ hr^{-1}\ ft^{-1}\ {}^{o}F^{-1}$ (British thermal units per hour per foot per degree Fahrenheit).

According to equation (3.0) above, the rate of conduction is proportional to the area of cross-section through which heat is transmitted and inversely proportional to negative of temperature gradient in the direction of heat flow. The area being perpendicular to the direction of heat flow. Thermal diffusivity **(κ),** is the ratio of thermal conductivity to the product of density and specific heat;

$$\kappa = \frac{\Lambda}{DC} \qquad (3.1)$$

where, Λ= thermal conductivity,

D= density of the material,

C= specific heat.

3.1 Theory of heat transfer

In this section and the next we try to answer two questions regarding thermal transfer; i.e., how heat is transferred and the quantity of heat transferred through matter.

The first question opens up an interesting idea that is becoming increasingly important now that material science and technology are reaching a point where, within limits, desired properties can be designed into the material. The second question is more or less important to engineers and applied scientists.

Heat transfer is a process that predicts the transfer of energy from one body to another or from one point to the next in the same body by virtue of temperature difference (Arora, 1989). As in any other form of energy transfer, there must be a potential difference in the heat transfer. It is evident from the second law of thermodynamics that "heat cannot flow from a body at low temperature to another

EGERTON UNIVERSITY LIBRARY

body at higher temperature without employing external work" (Helsdon, 1965; Finn, 1993). Thus heat must flow from high to low temperature regions until equilibrium is attained.

3.1.1 Modes of heat transfer

There are three modes of heat transfer; conduction, convection and radiation.

(i) Conduction

This is the term applied to the mechanism of internal energy exchange from one body to another or from one part of a body to another part by exchange of the kinetic energy of the molecules by free electrons (in metals) and phonon transfer (Chapman, 1984). This flow of energy or heat, passes from the higher energy molecules to lower energy molecules. The distinguishing feature of conduction is that it takes place within the boundaries of a body or across the boundary of a body into another body in contact with the first, without an appreciable displacement of the matter comprising the body, (Touloukian, 1970).

(ii) Convection

This is the term applied to the heat transfer mechanism which occurs in a fluid by the mixing of one portion of the fluid with another due to gross movements of the mass of the fluid (Chapman, 1984). There are two types of convection;

(a) Forced convection, where fluid motion is caused by an external mechanism such as a fan or pump. The circulation of water in a water tube boiler , shell and tube condenser of a refrigerator etc., are examples of forced convection. Other examples here include, car radiator, cooled condenser of an air conditioner.

(b) Natural convection, in which the fluid motion is caused by density differences which are created by the temperature differences existing in the fluid mass. An example is the circulation of water in a pan heated on a stove.

(iii) Radiation

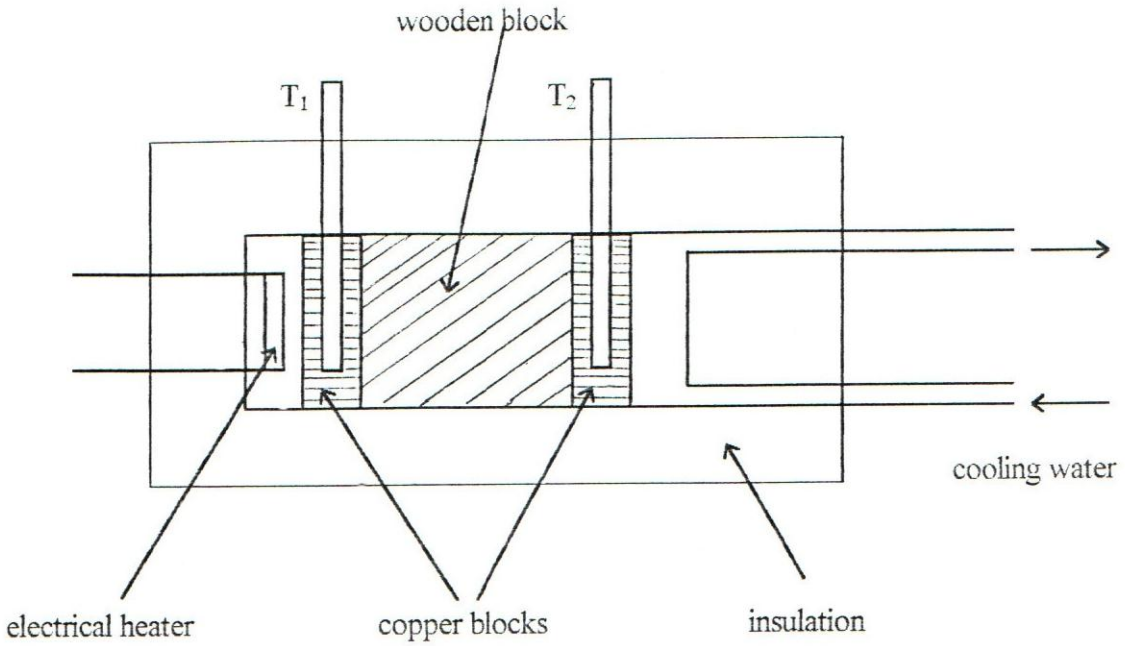
Thermal radiation is the term used to describe the electromagnetic radiation which is from the surface of a body that is thermally excited. This electromagnetic radiation is emitted in all directions, and when it strikes another body, part of it may be reflected, transmitted or absorbed. If the incident is thermal radiation ,of appropriate wavelength, the absorbed radiation will appear as heat within the absorbing body.

3.2 Methods of measurement of thermal conductivity

This section mainly deals with the answer to the question on how much heat is transferred through matter. Let us look at a small wooden block and assume that the block is homogeneous. For this elementary investigation of the rate of flow of heat, an experimental rig is designed to maintain one side of the block at a higher temperature than the other side, figure 3.1 below, (Cornwell, 1977).

Heat is supplied electrically to one side of the block and removed by a flow of cooling water on the other side. Temperature difference across the block may be measured by using thermometers T_1 and T_2 inserted in copper plates. Copper is used because it readily conducts heat and ensures that the temperature at the thermometer bulb is as near as possible to the temperature of the block face. The rate of heat flow through the block is found by measuring the power out put of the electrical heater or by measuring the increase in temperature of the water and its flow rate.

Fig. 3.1 Measurement of thermal conductivity of a piece of wood.



Experiments have shown that for such arrangements the rate of flow of heat Q, is directly proportional to the area, A, of the block through which heat flowsand the temperature difference (T_1 - T_2), and inversely proportional to the thickness ΔX, of the block.

This proportionality is made an equality by the definition of a constant of proportionality Λ, (Chapman, 1984).

$$Q = \Lambda A \frac{T_1 - T_2}{\Delta X} \qquad (3.2)$$

Λ is the thermal conductivity of the material.

The understanding of the fundamental physical processes related to the transfer of thermal energy in porous materials is essential. The reliability of a particular method for determination of thermal conductivity depends upon several factors, i.e., speed of operation, the required accuracy, the physical nature of the material and the geometry of the available sample (Suleiman, 1994). However, in most methods the main concern is to obtain a controlled heat flow in a certain direction, so that the actual boundary conditions in the experiment agree with those assumed in theory.

The various methods used so far may be divided into two broad categories,

(Mohsenin, 1980);

(a) Those using steady or static state conditions of heat transfer,

(b) Those using the transient or dynamic state conditions of heat transfer. The steady state methods are accurate but expensive to maintain, while the non-steady state methods are less complicated and simpler to use, though not as accurate as the steady state methods. Each of these could be divided into subcategories depending on the actual experimental and boundary conditions. These subcategories include a number of experimental techniques. In some of the methods, thermal diffusivity, heat capacity and surface conductance can also be obtained either directly or by calculations.

3.2.1 Steady state (static) methods.

The principle behind these methods is that the temperature gradient across the sample is invariant with time. Thermal conductivity of the sample is calculated directly using the equation below after thermal equilibrium has been attained;

$$J = -\sum_{j} \Lambda_j \frac{\partial T}{\partial x_j} \qquad (3.3)$$

where, J = current density in solids at steady state conditions,

Λ_j = thermal conductivity of the material, and

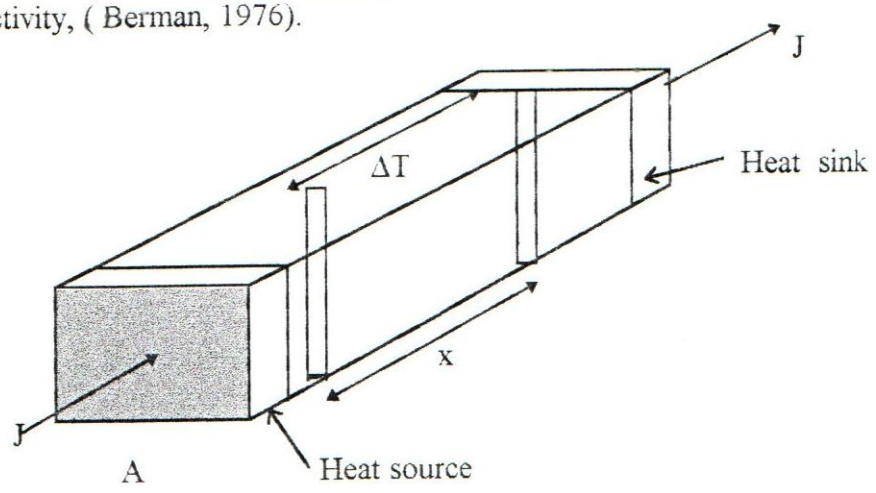
$$\frac{\partial T}{\partial x_j} \qquad (3.3.1)$$

is the temperature gradient in the j_{th} direction.

There are many categories of the steady state methods, (Berman, 1976), which include longitudinal heat flow, radial heat flow, electrical heating of the specimen and other comparative methods. The longitudinal and radial heat flow methods are the most common, they differ in the direction of heat flow and in the geometry of the sample.

(a) Longitudinal flow

Fig. 3.2 Principle of steady-state longitudinal heat flow method for measurement of thermal conductivity, (Berman, 1976).



Here, heat flows in the axial direction of the sample. The specimen is held longitudinally between a heat source and a heat sink. Heat is supplied at one end of a rod of uniform cross sectional area A at a known rate J and is removed at the other end. The temperature difference ΔT between two points along the specimen is measured using thermometers. These two points are at a distance x between each other. Conductivity is then derived from the equation;

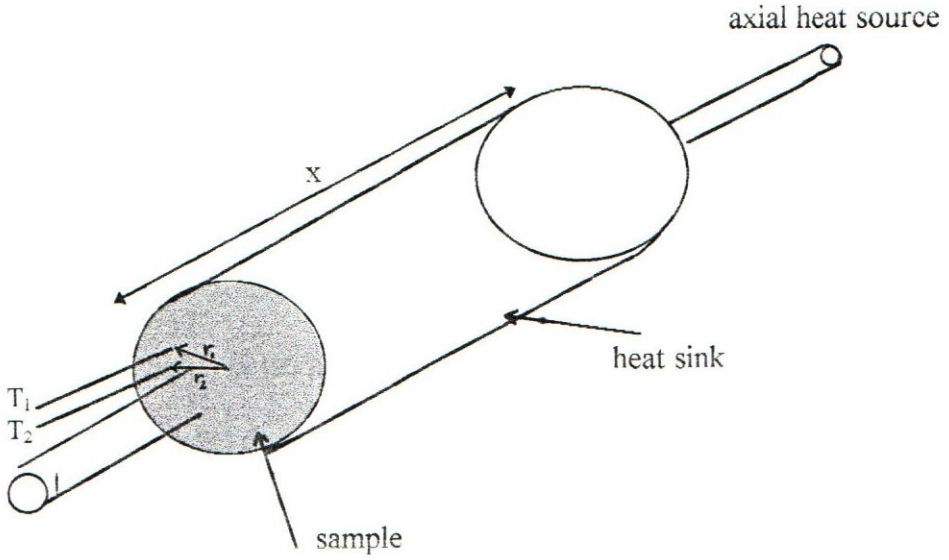
$$J = \Lambda A \frac{dT}{x} \qquad (3.4)$$

(b) Radial heat flow

In this case heat flows along the radial direction of the sample. A heating source is inserted along the axis of a cylindrical sample and provides heat uniformly along its length. The heat flow per unit length from inside to the outside is related to the temperatures T_1 and T_2 measured at the radii r_1 and r_2, by the equation;

$$\frac{Q}{x} = \frac{2\pi\Lambda(T_1 - T_2)}{\ln(\frac{r_2}{r_1})} \qquad (3.5)$$

Fig. 3.3 Principle of steady-state radial heat flow method of measurement of thermal conductivity.



This relationship holds for parts of the rod far from the ends where longitudinal heat flow is negligible, (Berman, 1976).

Due to this simplicity, steady state methods are widely used for large ranges of temperature. However at high temperatures, where heat losses become a problem, measurements have to be made under vacuum (Suleiman, 1994). Systematic errors could also arise due to other effects such as poor thermocouple contacts, temperature drift and thermal contact resistance.

3.2.2 Non-steady (Dynamic) state methods

The physical principle of these methods is that the temperature distribution in the sample varies with time. In general, an arbitrary temperature distribution set up in a body will change with time at a rate dependent on the ratio of thermal conductivity to the heat capacity per unit volume. This ratio is called thermal diffusivity.

$$\kappa = \frac{\Lambda}{C} \qquad (3.6)$$

These methods are applicable mostly for samples made of impure or composite materials, in order to obtain high accuracy in thermal conductivity. They are very important in many applications of heat transfer, such as in rocket nozzles, space re-entry walls, cooling and freezing of foods etc., (Arora, 1989).

As in the case of the static methods, heat can flow longitudinally or radially depending on the geometry of the sample in the dynamic methods. The advantages of these methods are; (i) they have shorter measuring (heating) time, (ii) there are lesser heat losses, (iii) heat losses can be included in the differential equation of heat flow or/ and in the boundary conditions, (iv) they are more frequently used at higher temperatures when a shorter heating time is often preferred in order to reduce heat losses and prevent changes that might occur in the structure of the sample.

Non-steady state methods are divided into two major categories (Arora, 1989; Suleiman, 1994);

(a) Periodic or Angstrom methods. The temperature at one end of the sample is made to vary sinusoidally and the attenuation of the temperature excursions and the time lag along the sample are determined.

If at x = 0, the temperature difference T^1 between the rod and its mean temperature varies with time as;

$$T^1(0) = T_0^1 \, \mathrm{Sin}(\omega t), \qquad (3.7)$$

then for no heat losses from the sides of the sample, the temperature difference from the mean at a distance x along the sample is;

$$T^1(x) = T_o^1 \exp[-(\frac{\omega}{2\kappa})^{1/2} x] \sin\{\omega t - (\frac{\omega}{2\kappa})^{1/2} x\} \qquad (3.7.1)$$

Under the ideal condition envisaged, the thermal diffusivity κ, could be determined either from the attenuation of the wave,

$$\frac{1}{\Lambda_{(x)}} = \exp\{-(\frac{\omega}{2\kappa})^{1/2} x\} \qquad (3.7.2)$$

or from the phase lag;

$$\psi_x = (\frac{\omega}{2\kappa})^{1/2} x \qquad (3.7.3)$$

where ψ is the phase angle.

so that,

$$\kappa = \frac{\omega x^2}{2(\ln \Lambda)^2} - \frac{\omega x^2}{2\psi^2} \qquad (3.7.4)$$

Fourier analysis solutions are necessary in the cases when measurements are performed close to the heated end of the sample and pure wave forms are not possible to achieve.

(b) Transient methods, where the thermal energy is supplied to the sample as a single addition or subtraction. The sample is initially at thermal equilibrium with the surroundings. The change in temperature is monitored at one or more points during the time of measurement. A simple relation between time taken to attain half the maximum temperature rise $T_{1/2}$, the thickness of the heating plate d and the thermal diffusivity is given by the equation; (Berman, 1976)

$$\kappa = \frac{1.37\, d^2}{\pi^2 T_{(1/2)}} \qquad (3.8)$$

In these transient methods, we have the line heat source methods in which a line heat source, either a wire or strip is embedded in the sample initially at uniform temperature, and the temperature rise measured at a given distance from the source after a short heating time (Mohsenin, 1980). If both the temperature changes and heat input are measured, the thermal conductivity and thermal diffusivity can simultaneously be determined (Suleiman, 1994).

Thermal conductivities of insulating materials, e.g., wood ash and vermiculite have been determined using the thermal probe method, (Aduda, 1987). Investigations on variations of

thermal conductivity with factors such as porosity, pore orientation to the heat flow, particle size and shape, volumetric concentration, and temperature were made. The study found that, among other variations, thermal conductivity decreased with increase in particle size in their lower range, and eventually increased with particle size in their higher range. It was also noted that thermal conductivity decreased as porosity increased.

The thermal or cylindrical probe method is essentially based on local behaviour of the thermal flow around a line heat source. A cylindrical metallic conductor is surrounded by an 'infinite' sample, such as soil or rock of much lower thermal conductivity. To a good approximation, the metal is regarded as a perfect conductor of heat. It has been found that in most problems interest is centred on the temperature of the material within the cylinder, leaving out the temperature of the surrounding (Mohsenin, 1980).

A study for determination of thermal conductivity of soils using an instrument based on the cylindrical probe method was made by Nicolas et al, (1993). The method appeared well suited to powdered materials though its application could be extended to viscous liquids and solid matter. The cylindrical probe was used to characterise nine soils from the Belgian Lorraine, (Nicolas et al, 1993). After soil analysis in the dry state, thermal conductivity of each was determined for different moisture contents.

In determination of thermal conductivity of soils, Baver et al, (1972) noted that steady state methods had two major weaknesses; it was subjected to the redistribution of water under the influence of a temperature gradient and it could not be used 'in situ'. The transient state cylindrical probe (Jackson, 1979), overcame these difficulties. This method basically consists of a thin metal wire that is electrically heated to serve as the heat source and a thermocouple to

measure temperature. There is radial flow of heat from the wire into the sample. Thermal conductivities are obtained using the equation below; (Mohsenin, 1980).

$$T - T_0 = \frac{Q}{4\pi\Lambda d} + \ln(t + t_c) \qquad (3.9)$$

where, T_o is the temperature at time t_0 ,

T is the temperature at time t,

Q is heat developed (per unit time and length of the source),

d is the diameter of heat source (a constant),

t is the time at the end of heating period,

t_c is a correction constant that depends on the probe as well as the thermal properties of both the probe and the sample.

Converting natural log. in equation (3.9) to log. base 10, thermal conductivity is obtained from the gradient by;

$$\Lambda = 2.303\frac{Q}{4\pi S} \qquad (3.9.1)$$

where, S = measured slope of graph of (T - T_0) versus log ($t + t_c$), (on a semi-log scale),

$\frac{Q}{4\pi S}$ is obtained from current (A) applied to the wire and the measured resistance per unit length (ohm per cm) of the probe.

Due to the theoretical assumption i.e., (i) infinitesimally thin line source and (ii) infinitely long line source, corrections for the probe diameter, axial heat flow and finite sample size have to be taken into account. In most cases these are accounted for through the term t_c.

Determination of thermal conductivity and thermal diffusivity of some building materials using the transient hot-strip method (THS) was done by Singh et al, (1985). In their study, the transient hot strip method developed by Gustafsson et al, (1979), for measurement of thermal conductivity and diffusivity of solids and fluids, was applied to dry dune sand, dry brick powder, cement, powdered mud and asbestos powder at room temperature and normal pressure. This hot-strip worked both as a temperature sensor and a heating element. The experimental values obtained for these materials were compared with those from thermal probe and hot wire methods. Good agreement in the values obtained indicated that the transient hot-strip method could also be used for loose porous materials.

In a study by Gustafsson et al, (1986), a thin electrically insulated layer was introduced between the hot-strip and the metallic material under study. The insulating layer introduces a certain thermal contact resistance between the hot-strip (heat source cum temperature sensor) and the surface of the sample being studied. To account for this thermal resistance, a theory was developed which indicates how measurements on these kind of materials should be performed and how the reduction of the data from transient recording should be carried out to give reliable results. According to this model, the thickness of the insulating layer was much less than the width of the hot strip and that its heat capacity could be neglected after a time t_0. The time varying resistance of the strip can be given as (Gustafsson et al 1989) ;

$$R = R_0 [1 + a(16\pi d^2 h\Lambda)^{-1} \int_0^t dt'Q(t')\psi(t,t')] \qquad (3.10)$$

where, $$\psi(t,t') = (t - t')^{-1} \int_{-d}^{d} dy \int_{-d}^{d} dy' \exp(-(y - y')^2 [4k(t - t')^{-1}] \qquad (3.10.1)$$

α = the temperature coefficient of resistivity (TCR) of the strip.

Using the mean-value theorem for integrals (Stroud, 1986), we can find a correction time (t_c) such that;

$$\int_0^t dt' Q(t')\ \psi(t,t') = P_0 \int_{t_c}^t dt' \psi(t,t') \qquad (3.10.2)$$

and consequently,

$$R = R_0 \{1 + \alpha P_0 (16\pi d^2 h\Lambda)^{-1} \int_{t_c}^t dt' \psi(t,t')\} \qquad (3.10.3)$$

which is evaluated to; (Gustafsson et al, 1986),

$$R = R_0 [1 + \alpha P_0 (2\pi^{1/2} h\Lambda)^{-1} f(\tau_c)] \qquad (3.11)$$

Where the $f(\tau)$ function is defined as the solution to the heat equation and;

$$\tau_c = [(t - t_c)/\theta]^{1/2} \qquad (3.11.1)$$

The thermal probe theory

This is the theory from which the experimental set up in this study (chapter 4) is based. In this theory, the idea of transient heat flow in an infinite mass initially at uniform temperature and heated by a line source of constant strength is used. To understand the theory, consider an infinite homogeneous sample mass e.g. soil which is initially at uniform temperature. At time t = 0, heat is released by the source at a known constant rate Q_n, per unit of source length. This constant production of heat by the

line source embedded in the sample mass will produce a cylindrical temperature field. The temperature rise (ΔT) at any point in the sample mass will be a function of the probe and the time t.

For each case we have;

$$\frac{\partial T}{\partial t} = \alpha[\frac{\partial^2 T}{\partial r^2} + \frac{1}{r}\frac{\partial T}{\partial r}] \qquad (3.12)$$

subject to initial and boundary conditions;

$T = T_o$ for $t = 0$

$T = T_o$ at $r = \infty$, $t > 0$ (3.12.1)

$$Q_n = -\lim_{r \to 0} 2\pi\Lambda r \frac{\partial T}{\partial r}, \qquad \text{for } t \geq 0 \qquad (3.13)$$

where, T is the temperature at radial distance r, in °C,

t is the time in seconds,

r is the radial distance from heat source in cm.

The solution to equation (3.14) can be given by;

$$T = T_0 + \frac{Q_n}{4\pi\Lambda}\int_0^t \frac{e^{-r^2/4\alpha t}}{t} dt \qquad (3.14)$$

substituting, $U = \frac{r^2}{4\alpha t}$, we get,

$$T = T_0 - \frac{Q_n}{4\pi\Lambda} \int_{\infty}^{(r^2/4\alpha t)} \frac{e^{-u}}{u} du \qquad (3.14.1)$$

$$T = T_0 + \frac{Q_n}{4\pi\Lambda} \int_{(r^2/4\alpha t)}^{\infty} \frac{e^{-u}}{u} du \qquad (3.14.2)$$

$$T = T_0 - \frac{Q_n}{4\pi\Lambda} Ei(\frac{-r^2}{4\alpha t}) \qquad (3.14.3)$$

where, $$-Ei(\frac{-r^2}{4\pi t}) = \int_{(r^2/4\alpha t)}^{\infty} \frac{e^{-u}}{u} du, \qquad (3.14.4)$$

is an exponential integral.

For small values of $(r^2/4\alpha t)$ corresponding to large values of time or small radii, the exponential integral may be approximated by series expansion as follows, (Log, 1993; Stroud, 1986);

$$-Ei(\frac{-r^2}{4\alpha t}) \cong \ln(\frac{4\alpha t}{r^2}) - \frac{r^2}{4\alpha t} + \frac{1}{4}(\frac{r^2}{4\alpha t})^2 + \ldots - \beta \qquad (3.14.5)$$

Where β is Euler's constant.

By neglecting terms of the order 1/t and higher, this series can be approximated to;

$$-Ei(\frac{-r^2}{4\alpha t}) = \ln(\frac{4\alpha t}{r^2}) - \beta \qquad (3.14.6)$$

So that,

$$T = T_0 + \frac{Q_n}{4\pi\Lambda}[\ln t + \ln(\frac{4\alpha}{r^2}) - \beta \qquad (3.15)$$

If T_1 and T_2 be the temperatures at times t_1 and t_2 respectively at a given point in the medium, equation (3.15) becomes,

$$T_2 - T_1 = \frac{Q_n}{4\pi\Lambda}[\ln \frac{t_2}{t_1}] \qquad (3.15.1)$$

or, $$T_2 - T_1 = \frac{2.303}{4\pi\Lambda} Q_n \log(\frac{t_2}{t_1}) \qquad (3.16)$$

It is possible to calculate Λ if the temperature rise at only two experimental times is known. The slope of the straight line graph of $(T_2 - T_1)$ Vs $\log (t_2/t_1)$ is given by;

$$S = \frac{2.303}{4\pi\Lambda} Q_n \qquad (3.16.1)$$

This equation enables us to calculate thermal conductivity of the sample from the known value of heat produced per cm length of the wire, Q_n, given by;

$$Q_n = \frac{I^2 R}{J} X10^7 = 0.24 I^2 R \qquad (3.17)$$

where, I is current in Amperes,

R is the resistance in ohms (Ω),

J is the equivalent heat.

It may be noted that the value Λ does not depend upon the radial distance r at which measurements of temperature are made.

Variations of the line heat source method are the transient hot wire (THW) method as used by Log (1993), and the transient hot strip (THS) method initially introduced by Gustafsson (1979). The next section has been devoted to the THS method which is the main experimental method in this work.

3.2.3 The Transient-Hot Strip (THS) Method.

This method is based on transient temperature rise of a thin metal foil at constant energy input. First developed by Gustafsson et al, (1979), the method was used for simultaneous measurement of thermal conductivity and thermal diffusivity of solids and fluids with low electrical conductivity. The strip works both as a heat source and a temperature sensing device. Measurements are performed by recording the voltage, resistance or temperature variations across the strip while exposing it to a constant electrical pulse. The measurement time is usually in the order of a few seconds.

The variation of voltage (V) between the ends of the metallic strip during the transient recording is given by the equation, (Gustafsson et al, 1979; 1986);

$$V = V_0[1 + \frac{\alpha P_0}{4\pi^{1/2}\Lambda h} f(\gamma)] \qquad (3.18)$$

where, α is the temperature coefficient of resistivity (TCR) of the material of the strip,

P_0 is the total power out put per unit length of the strip,

V is the instantaneous voltage at time t, across the strip,

V_0 is voltage across the strip before transient recording has been initiated,

Λ is the thermal conductivity of the sample and,

$$f(\gamma) = \gamma erf(\frac{1}{\gamma}) - \frac{\gamma^2}{2\pi^{1/2}}[1 - \exp(-\gamma^{-2})] - \frac{1}{2\pi^{1/2}}[-Ei(-\gamma^{-2})] \qquad (3.18.1)$$

which is the theoretical expression describing the solution to the heat equation, assuming a plane heat source with a negligible thickness and h >> d, where 2d and 2h are the strip width and length respectively.

The f(γ) function has to be analytically approximated for small values of γ, while for γ values larger than, say, 0.3 it has to be evaluated numerically (Gustafsson, 1991). This is readily done with a microcomputer. For mathematical convenience f(γ) is defined in terms of the non-dimensional variable,

$$\gamma = (\frac{\kappa t}{d^2})^{1/2} = (\frac{t}{\theta}) \qquad (3.18.2)$$

where,

κ = thermal diffusivity of the sample,

t = time measured from start of transient heating,

θ = characteristic time.

We also have the functions erf and Ei. The erf is called the error function defined by;

$$erf(u) = (2\pi)^{-1/2} \int_u^{\infty} \exp(-x^2) dx \qquad (3.18.3)$$

which can be simplified using the power series expansion for the exponent (Thomas, 1995), as below;

$$erf(u) = \frac{2}{\pi^{1/2}}(u - \frac{u^3}{3} + \frac{u^5}{10} - \ldots) \qquad (3.18.4)$$

and in terms of γ,

$$erf(\gamma^{-1}) = \frac{2}{\pi^{1/2}}(\frac{1}{\gamma} - \frac{1}{3\gamma^3} + \frac{1}{10\gamma^5} - \ldots) \qquad (3.18.5)$$

and Ei is called the exponential integral expressed as;

$$Ei(u) = \int_u^{\infty} x^{-1}\exp(-x^2)dx \qquad (3.18.6)$$

and from our equations (3.9.1) and (3.9.3), simplification of the exponential integral is;

$$-Ei(-\gamma^{-2}) = \ln\frac{1}{\gamma^{-2}} - \gamma^{-2} + \frac{1}{\gamma^{-4}} + \ldots - \beta \qquad (3.18.7)$$

where, β is called Euler's constant (β = 0.5772156).

This expression for error function is true for small values of γ corresponding to small values of t or large values of θ as in the case with this study. Different values of t and θ have been used to obtain

corresponding values of f(γ), (Appendix IV, page 103). In this work, the simplified expression for f(γ) that has been used for calculations is,

$$f(\gamma)=\frac{1}{2\pi}[4+\ln(\frac{t}{\theta})-\frac{11}{60}(\frac{\theta}{t})+\frac{29}{60}(\frac{\theta^2}{t})+....-\beta] \qquad (3.19)$$

Equation (3.9) may be re written as ;

$$V=V_o+Cf(\gamma_i) \qquad (3.20)$$

where, $$C=\frac{\alpha V_o P_o}{4\pi^{1/2}h\Lambda} \qquad (3.21)$$

A plot of V_i versus $f(\gamma_i)$ will give a straight line if θ has its correct value. It is possible to find the correct value of θ using an iterative procedure by varying θ, (Log, 1993),until the correlation coefficient for the straight line fit of V_i against $f(\gamma_i)$ reaches its maximum value (≅ 1).

Then thermal diffusivity can be calculated from;

$$\kappa = d^2/\theta \qquad (3.21.1)$$

once θ is determined. Thermal conductivity can also be calculated from the gradient, C, of the graph of V_i versus f(γ).

3.3 Factors affecting thermal conductivity of porous systems

Experimental observations indicate that thermal conductivity depend upon factors like texture of the material, porosity or compaction, moisture content, mineralogical composition, size of particles and their distribution and temperature (Ghildyal and Tripathi, 1987). According to Aduda, (1987) thermal conductivity also depends on volumetric concentration of the various constituents and interstitial air pressure, overburden pressure (mechanical load) and saturating medium.

(a) Texture and particle size

The general trend of thermal conductivity is that it decreases with reduction of particle size. For example, the thermal conductivity of Carborundum is lowered by about 70 % as the particle size is reduced from 450 to 6μm, while that of quartz particles reduces from about 1/51 to 1/20 of the solid quartz particles (Ghildyal and Tripathi, 1987). Reduction of thermal conductivity with fineness of the texture is normally associated with the reduced area of contact between the particles (Kanan, 1989; Kinyanjui, 1995).

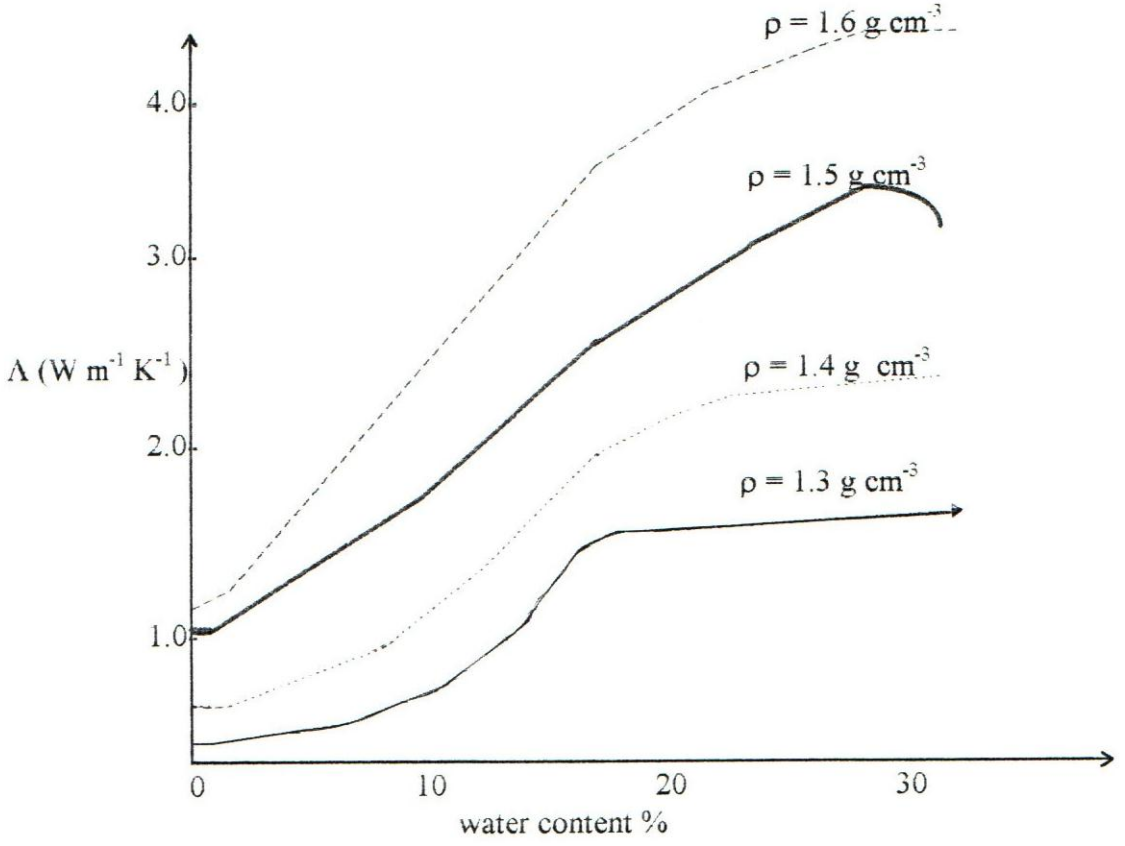
For granular materials it has been shown that at elevated temperatures, thermal conductivity rises with increasing particle size due to radiant heat transfer through the voids, and internal pores between and in the particles (Bever, 1986).

(b) Moisture content

There is considerable variation of thermal conductivity of porous materials with moisture content. For example figure 3.4 shows that there is a slow rate of increase of thermal conductivity for

values below 7 % and above 20 % moisture content. But in between 7 % and 20 % moisture content, this increase is very rapid. Beyond 20 %, thermal conductivity becomes stable. It is also seen that at a particular moisture content, thermal conductivity of the porous samples increases with increase in density as a results of closeness of particles.

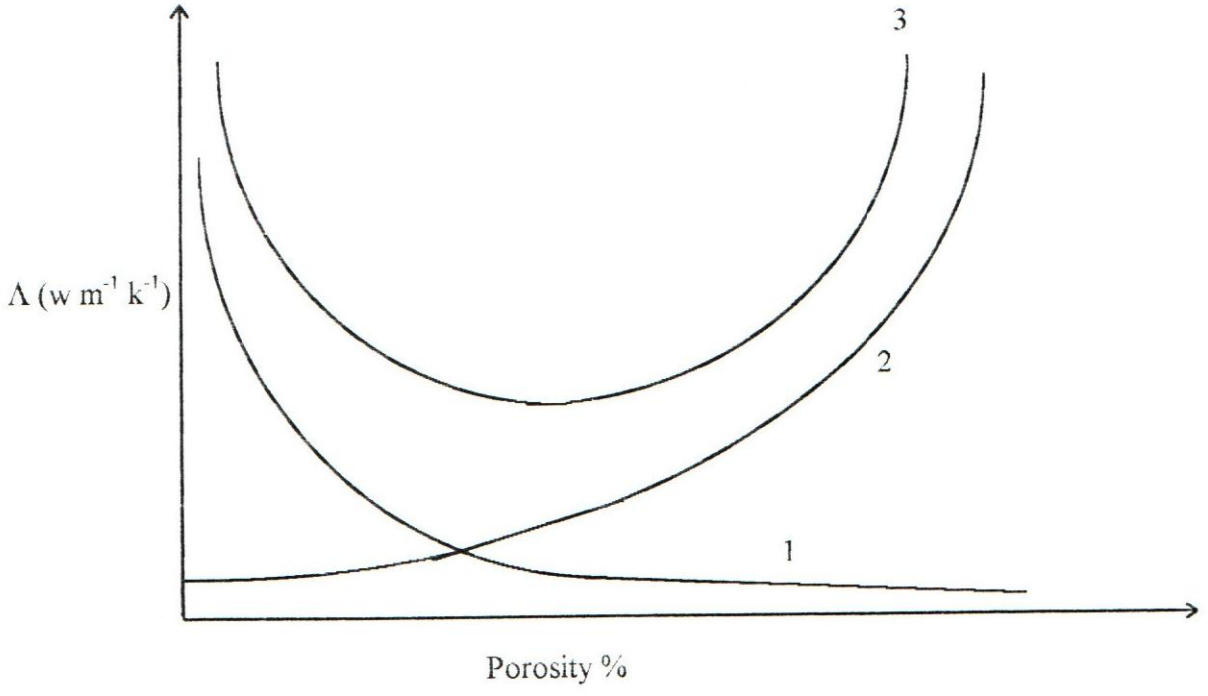
Fig. 3.4 Showing that thermal conductivity (Λ) per unit of water added in silty loam soil increases gradually at low (< 7 %) and high (> 20 %) water contents, but increases rapidly between 7 % and 20 % water content. After (Ghildyal and Tripathi, 1978).



(c) Compaction and porosity

Thermal conductivity of consolidated samples is often found to increase with compaction. In a dry sample, the increase in thermal conductivity with compaction is normally associated with decreased porosity and thus the air content, and increased thermal contact between the particles. In sands, for example a 50% decrease in porosity has been found to result in approximately two fold increase in the thermal conductivity and approximately 33% increase in thermal diffusivity (Ghildyal and Tripathi, 1987).

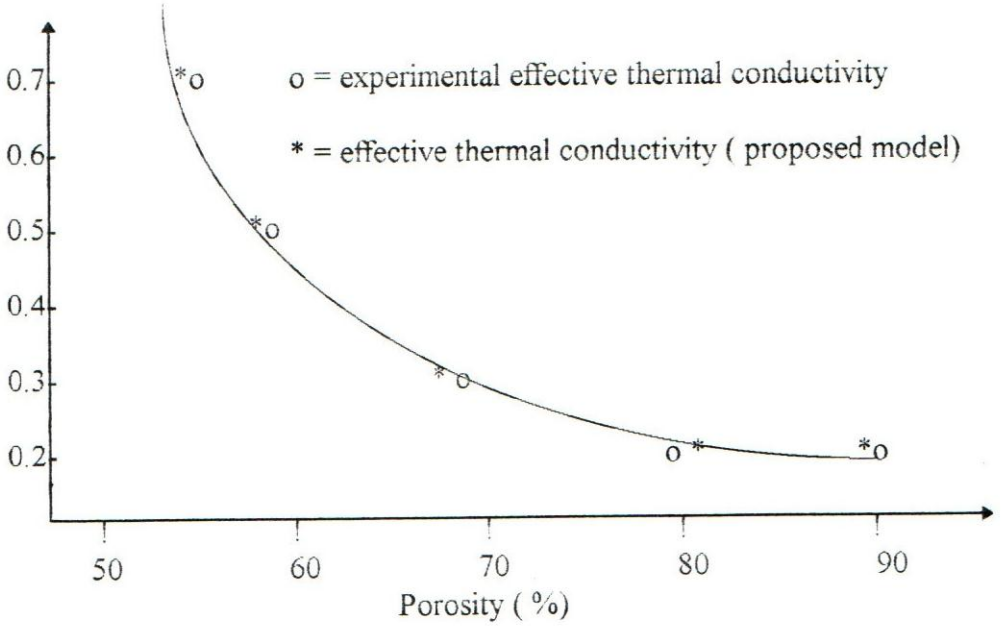
Fig 3.5 General variation of thermal conductivity with porosity for most powders. (After Fountain and West, 1970)



Curve 1 indicates a graph typical of refractory and insulating powders. There is decrease in conductivity as porosity increases. This is due to enhanced conduction through the solids at low porosity. Curve 2 indicates what is expected of granular substances at elevated temperatures. When radiative heat is dominant, there is general increase of thermal conductivity with increase in porosity. Curve 3 is typical of a medium in which at low and moderate temperatures, heat transfer through solid conduction dominates but at high temperatures radiative heat transfer becomes dominant. Such a curve is expected of powders which are continually packed to reduce porosity.

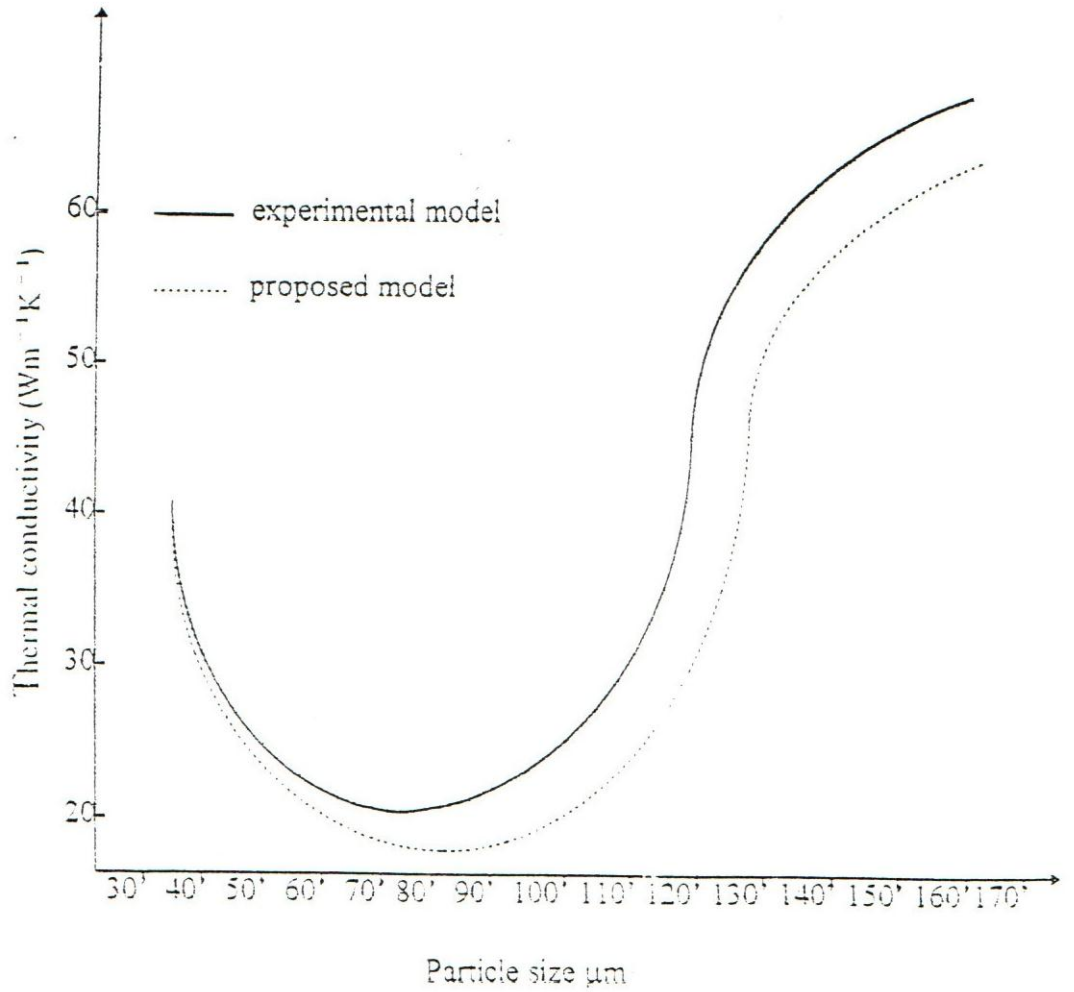
Kanan et al, (1989), experimentally measured thermal conductivity of copper powders for different particle sizes at room temperature and normal pressure using the transient hot-strip method. A variation in the values of the effective thermal conductivity of these powders with their porosity was observed and is summarised by figure 3.6 below.

Fig. 3.6 Variation of effective thermal conductivity of copper powder samples with porosity, (After Kanan et al, 1989).



The results show that the effective thermal conductivity of copper powder decreased as the porosity of the samples increased. This is due to the presence of increased voids in the sample. Effective thermal conductivity has a slight decrease in the low particle size range where voids are limited , then increases as particle size increases. This shows that there was agreement between theoretical and experimental values for copper powders of all particle sizes. The figure below summarises this.

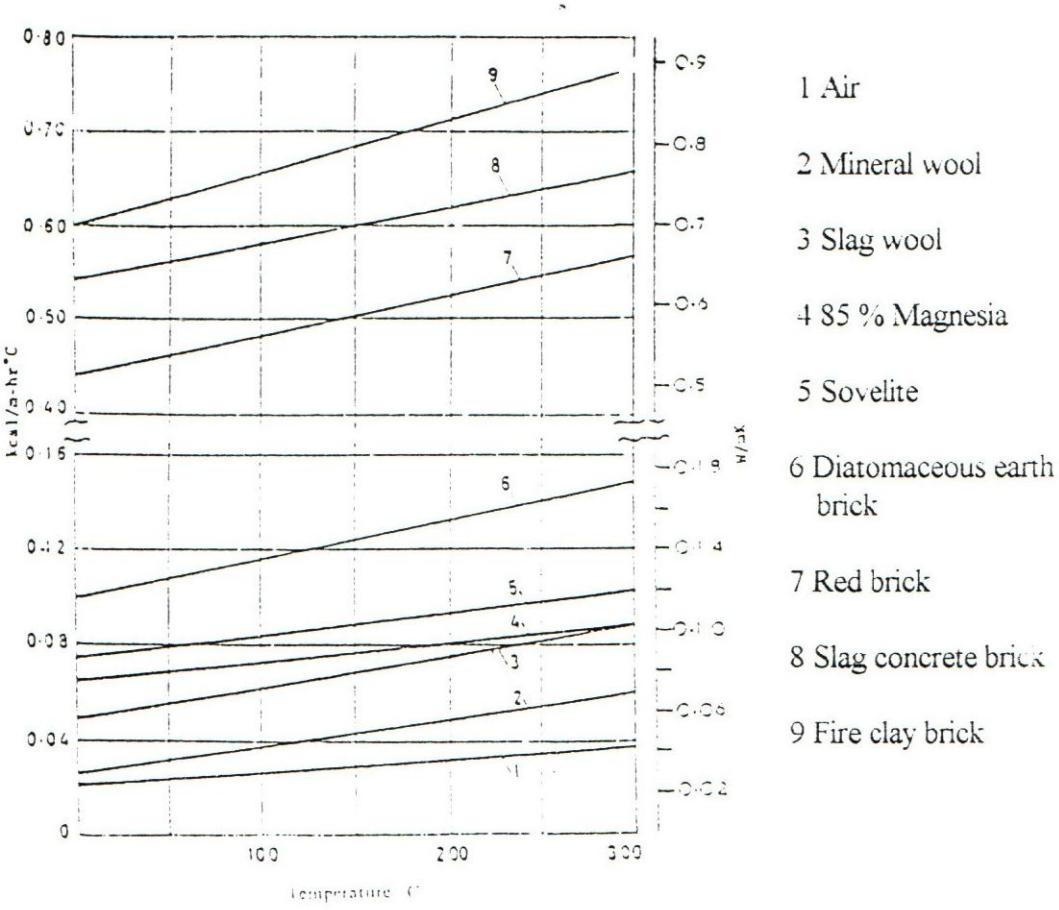
Fig 3.7 Variation of effective thermal conductivity of copper powder with particle size. (After Kanan et al, 1989)



(d) Temperature

Most metals show a general decrease of thermal conductivity as temperature is increased, but for different thermal insulating and refractory materials, increase in temperature shows a general increase in thermal conductivity (Subramanyam and Kothandaraman, 1989)

Fig 3.8 Variation of thermal conductivity of different materials with temperature.(After Subramanyam and kothandaraman, 1989)



1 Air

2 Mineral wool

3 Slag wool

4 85 % Magnesia

5 Sovelite

6 Diatomaceous earth brick

7 Red brick

8 Slag concrete brick

9 Fire clay brick

3.4 Theoretical models for prediction of thermal conductivity

So far, vast experimental materials have been accumulated and many formulae have been proposed for the prediction of the effective thermal conductivity of porous systems. Porous systems can be conventionally divided into solid porous materials with definite shape, granular materials and fibrous materials. The reported data on thermal conductivity of pure materials (crystals and amorphous solids, metals, gases, fluids) are rather numerous (Luikov et al, 1966). For porous systems composed of pure substances, thermal conductivity depends on the properties and volumetric proportions of the pure materials they include. The knowledge of thermal properties and interaction between the elements in the heterogeneous systems allows thermal conductivity of such systems to be calculated.

3.4.1 Wimmer's model (Kanan et al, 1989)

This model considers the powdered system as a solid consisting of a lattice of microcrystallines from which certain lattice points are missing. These points create voids in the system. The measured value of effective thermal conductivity (Λ_{eff}) is connected with the theoretically dense value of thermal conductivity (Λ_{TD}), which is independent of porosity and is given as; (Kanan et al, 1989),

$$\Lambda_{TD} = \Lambda_{eff} \frac{(1 - 0.5\rho)}{(1 - \rho)} \qquad (3.22)$$

where ρ is the porosity of the sample having an effective thermal conductivity Λ_{eff}.

In all practical cases, where the systems are composed of different particle sizes, we observe that the porosities have different values. The value of effective thermal conductivity Λ_{eff}, is reduced from Λ_{TD}. This is due to the presence of voids and can be accounted as follows;

We consider N solid particles present in a volume V_s in the theoretically dense system, then the area occupied by a particle in a given section will be;

$$A \propto (\frac{V_s}{N})^{2/3} \qquad (3.23)$$

Hence the number of particles per unit area, normal to the direction of heat flux is given by;

$$n_s \propto \frac{1}{A}(\frac{N}{V_s})^{2/3} \qquad (3.24)$$

In the case of powders consisting of solid particles and voids, with porosity $\rho = 1 - Vs/V$, the same number N of solid particles will now occupy a volume V and the area occupied per particle will be;

$$A \propto (\frac{V}{N})^{2/3} \qquad (3.25)$$

The number of particles per unit area normal to the heat flux, in this case is given as;

$$n \propto \frac{1}{A} \propto (\frac{N}{V})^{2/3} \qquad (3.26)$$

Thus due to the presence of voids, the probability of occupation of a given area normal to the flow of heat has been reduced by a factor;

$$\frac{n}{n_s} = (\frac{V_s}{V}) = (1-\rho)^{2/3} \qquad (3.27)$$

Let us now consider heat conduction. It will be possible to conduct heat through some sections only when a particle in one section is facing another in the other section. The probability of two particles occurring face to face in two successive sections and being responsible for heat flow by conduction is reduced by a factor of $(V_s/V)^2=(1-\rho)^{4/3}$ as compared to the probability when it was theoretically dense. Hence the effective thermal conductivity of the powder system in terms of Λ_{TD} can be expressed as, (Kanan et al, 1989);

$$\Lambda_{eff} = \Lambda_{TD}(\frac{V_s}{V})^{4/3}$$

$$= \Lambda_{TD}(1-\rho)^{4/3} \qquad (3.28)$$

3.4.2 The model of Luikov et al, (1966)

This model considers the application of the method of generalised conductivities for the determination of the effective thermal conductivity on the example of dry granular systems. The effective thermal conductivity of a granular system is expressed as a function of a number of parameters. The shape of real granular materials can be greatly diverse. The more defined the shapes of the particle the higher, in general, is the overall porosity of the material. Theoretically, the porosity of the most densely packed

tetrahedral arrangement is 26%, but experimentally the porosity of a granular system is approximately between 39% and 98%, (Luikov et al, 1966). Consider the sample in a rectangular cell. Let V be the total volume of an elementary cell, V_1 the volume of solid phase of the elementary cell and V_2 the volume of the gaseous phase. To establish the relationship between porosity and the ratio h/l, (h is the thickness and l is the length of one quarter of the cell), porosity can be expressed as;

$$\rho = f(h/l) \tag{3.29}$$

If the lines of heat flow are assumed to be parallel to the vertical generating lines of the unit cell, then thermal resistances of the components of the one-quarter cell can be presented as; (Luikov et al, 1966; Luikov, 1964),

$$R_1 = \frac{L}{\Lambda_s d^2}, \quad R_2 = \frac{2}{\Lambda_s l}, \quad R_3 = \frac{2}{\Lambda_g d}, \quad R_4 = \frac{4L}{\Lambda_g l^2}, \quad R^1{}_g = \frac{4h_r k_k}{\Lambda^1_g h^2}$$

$$R_c = R_L + R_{sp} + R_o \tag{3.30}$$

Let h = 2d, where h and d are the thickness and the width of the skeleton cell respectively; R_L the resistance determined by narrowing the lines of heat flow in the region adjacent to the place of contact; R_{SP} the resistance of the microroughness at the place of contact; R_o the resistance of the oxidic film. The effective thermal resistance of the one-quarter cell is;

$$R_{eff} = \frac{4}{\Lambda_{eff} L} \tag{3.31}$$

Similarly, thermal conductance can be presented as;

$$\sigma_1 = \frac{1}{R_1 + \dfrac{4}{\sigma^1_g + \sigma_c}}; \quad \sigma_2 = \frac{\Lambda_g l^2}{4L}; \quad 2\sigma_3 = \frac{1}{R_2 + \dfrac{R_3}{2}};$$

$$\sigma_g^1 = \frac{\Lambda_g^1 h^2 10^3}{4Lk_m k_k} \; ; \qquad \sigma_c = \frac{1}{R_L + R_{sp} + R_o} \tag{3.32}$$

The effective thermal conductance is;

$$\sigma_{eff} = \sigma_1 + \sigma_2 + 2\sigma_3 \tag{3.32.1}$$

If the corresponding value of conductance are substituted into equation (3.32.1) then we shall obtain;

$$\frac{\Lambda_{eff} L}{4} = \frac{1}{\frac{4L}{\Lambda_s h^2} + \frac{4}{\sigma_c + \sigma_g^1}} + \frac{\Lambda_g l^2}{4L} + \frac{1}{\frac{2}{\Lambda_s l} + \frac{2}{\Lambda_g h}} \tag{3.32.2}$$

Simplifying we get the initial formula for calculation of the effective thermal conductivity of the porous system ;

$$\frac{\Lambda_{eff}}{\Lambda_s} = \frac{1}{\frac{1}{(h/l)^2} + A} + \nu_g (1 - h/l)^2 + \frac{2}{1 + (h/l) + \frac{1}{\nu_g h / L}} \tag{3.33}$$

where, $A = \dfrac{1}{\frac{\Lambda_c}{\Lambda_s} + \frac{\nu_g^1}{4k_k k_m}(\frac{h}{L})^2 .10^3}$; $\quad L = l + h$; $\quad \dfrac{h}{H} = \dfrac{(h/l)}{1 + (h/l)}$;

$$\nu_g = \frac{\Lambda_g}{\Lambda_s} \; ; \qquad \nu_g^1 = \frac{\Lambda_g^1}{\Lambda_s} . \tag{3.33.1}$$

From this model we see that there are four independent modes of heat transfer in porous particulate systems; (a) heat conduction directly through contact; (b) heat conduction through the medium filling the pores and the surface between the projections of roughness of the contact surfaces; (c) radiative heat transfer between surfaces; (d) gas convection in the pores.

CHAPTER 4

4.0 EXPERIMENTAL TECHNIQUES

This chapter describes the various experimental procedures used in this work. The methods used include, sieving for particle size measurement, measurement of porosity, preparation of sample into slabs and composites and measurement of thermal conductivity.

Samples of diatomite ore were supplied by The African Diatomite Industries (ADI -Kenya), of Gilgil in the Rift Valley of Kenya. The 'F' diatomite was mined at Kariandusi mines and the 'Bu' diatomite from Soysambu mines, both near Gilgil. F and Bu are the symbols used by ADI to distinguish between these two types of diatomite.

Wood ash samples were prepared by burning of saw dust and wood chips using the usual wood stove ('jiko'). Wood from the Mau forest in Njoro, also in the Rift Valley of Kenya ,were used. Burning was controlled (done completely) to ensure that only wood ash was collected and used in the experimentation.

4.1 Measurement of particle size

The size of a spherical homogeneous particle is uniquely determined by its diameter. For a cube, the length along one edge is the characteristic size, and for other regular shapes there are equally appropriate dimensions. In case of irregular particles it may be necessary to specify more than one dimension (Allen, 1990).

There are many methods of sizing material particles. These include, inspection methods, microscopy, sedimentation, X-ray diffraction and sieving.

The inspection or manual methods involve using hands and eyes to separate large particles from small ones. It is mainly applicable to very large particles. It is however tedious.

Microscopy is used as an absolute method of particle size analysis, since it is the only method where individual particles are observed and accurately measured. It also permits examination of the shape and composition of the particles with a sensitivity far greater than any other technique.

X-ray diffraction method requires that the X-ray beam diameter be greater than the grain (particle) diameter, and the grains be uniform in size, the grain size is the most distributing factor. However, particle size can be determined in the extremely fine size range by small angle scattering of X-rays, (Clark, 1940).

Sedimentation is the method applied to very fine particles. A well dispersed sample is placed in a liquid column and sampling is done at different time intervals. The concentration of the sample particles at a given depth in the liquid is determined as a function of time (Ghildyal and Tripathi, 1987). It is recognised that the rate of fall of the particles through a liquid medium is a function of particle size, density and shape, and the viscosity of the medium. The larger the particle the faster is the rate of settling.

Sieving is an obvious method for particle size classification. It is an important technique since particles are sorted into categories on the basis of size alone independent of other properties of the material (Allen, 1990). It can also be used to classify dry powder particles and produce narrowly classified fractions.

In this study the sieving method was used. In measurement of particle sizes machine sieving was used. Here sieves were stacked in order of mesh size:- i.e., 1000 μm, 500 μm, 100 μm, 74 μm, and 45 μm. The sample particles were poured onto the topmost sieve (1000 μm) and a lid placed to

prevent loss of particles. A receiving pan was placed at the bottom of the stack for the finest particles. The whole stack was vibrated mechanically at a constant rate for a fixed time of 30 minutes. This time was chosen to be long enough to give the particles time to pass through the appropriate sieves. The residual weight of the particles on each sieve was determined and expressed as a percentage in terms of the normal sieve aperture (as discussed in chapter 5).

4.2 Determination of density and porosity

4.2.1 Bulk density

Bulk density of porous materials is defined as the ratio of the mass to the bulk volume of the particle with pore spaces of the sample included. The total mass is determined after drying the sample to a constant weight at 105 °C. The volume is taken as that of the sample or simply that of the sample container. Bulk density is calculated using the expression; (Black, 1965),

$$D_b = \frac{M_s}{V_b} \qquad (4.1)$$

where, M_s is the mass of the solid particles oven dried at 105 °C for 4 hours

(assuming no contribution of air to bulk density),

V_b is the bulk volume (volume of sample holder);

V_b = total volume of sample + volume of air spaces

4.2.2 Measurement of particle density of unconsolidated sample

Particle density is the ratio of total mass of solid particle to the total volume they occupy, excluding pore spaces between the particles . The mass is determined by weighing the dry sample, while the volume is determined by the calculation from the mass and density of water or any other fluid displaced by the sample. For porous systems particle density is important since porosity, bulk density, rate of sedimentation of the particles as well as particle movement depend upon it.

For unconsolidated or granular sample, particle volume is measured using a pycnometer (specific gravity bottle).

Particle density is calculated using the expression; (Black et al, 1965),

$$D_\rho = \frac{d_\omega (W_s - W_a)}{(W_s - W_a) - (W_{s\omega} - W_\omega)} \qquad (4.2)$$

where, d_ω is the density of water displaced by sample,

W_s is the weight of pycnometer with sample,

W_a is the weight of pycnometer filled with air,

$W_{s\omega}$ is the weight of pycnometer with sample and water,

W_ω is the weight of pycnometer filled with water.

The total porosity which is defined as a percentage of the bulk volume not occupied by the solid particles was then calculated using the expression;

$$\rho = [1 - \frac{D_b}{D_p}] \times 100\% \qquad (4.3)$$

4.3 Preparation of sample composites

Granular samples of wood ash, Bu and F diatomite were dried overnight at 105 °C to improve their friability. The mixture of the samples was poured into a mixing apparatus and mixed for 30 minutes. This length of time ensured homogeneity of the dry mixture.

The proportion by mass of the composite mixture was made as shown in Tables 1 to 4 below;

(a) Preparation of composite comprising of only two pure samples A and B.

In this case, either, A is Wood ash and B is 'F' diatomite, or A is Wood ash and B is 'Bu' diatomite, or A is 'Bu' and B is 'F' diatomite. Each mixture was made into a percentage ratio by mass of the two pure samples A and B as shown in Table 1 below;

Table 1 Composite mixture of only two samples

Sample A	Sample B
100%	0%
75%	25%
50%	50%
25%	75%
0%	100%

(b) Preparation of composites comprising of all the 3 pure samples WA, Bu and F.

In this case, each composite mixture had one of the three pure samples kept constant by mass. This was necessary in order to monitor the contribution of the other two samples in the mixture. The composite mixtures were made in the following percentage by mass;

Table 2. Composite mixtures of Bu, F diatomite samples with WA constant, (see Table 8).

WA % mass	Bu % mass	F % mass
50	40	10
50	30	20
50	20	30
50	10	40

Table 3. Composite mixtures of Bu, WA with F constant, (see Table 9).

Bu % mass	F % mass	WA % mass
10	50	40
20	50	30
30	50	20
40	50	10

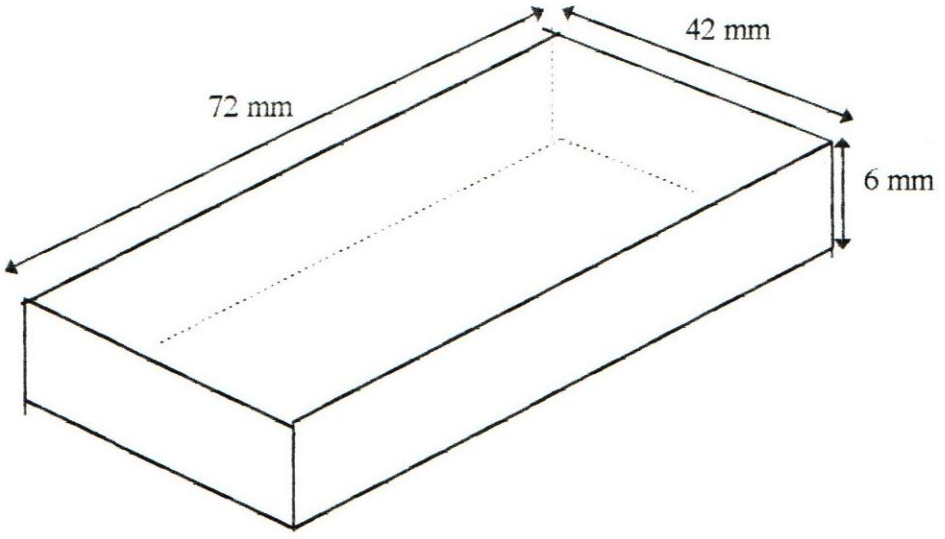
Table 4. Composite mixture of F, WA with Bu constant, (see Table 10).

F % mass	WA % mass	Bu % mass
40	10	50
30	20	50
20	30	50
10	40	50

4.4 Slab preparation (Consolidated sample)

A slab moulding box of dimension 42 mm x 72 mm x 6 mm was made from plastic. One of its sides was left open to allow removal of the slabs after setting.

Fig 4.1 Plastic slab moulding box.



Unconsolidated samples were mixed with distilled water to obtain a mix of sufficient plasticity, then poured into the moulding box. Pressing was done using different compacting forces (see section 4.5) and the mould removed from the box. The slab was left to set in the sun.

4.5 Determination of porosity of consolidated sample

The difference in porosity for consolidated samples comes as a result of variation in general, of compaction of the samples. In this case the samples of wood ash , diatomite and their composites were compacted using different compacting forces of 0.2 N, 0.4 N, 0.6 N, and 0.8 N, as the volume of the slabs was kept constant. In order to measure the porosity, each of these slabs was weighed when completely dry, and the weight noted. The slab was then placed in a beaker of water. After about 20 minutes, (enough time for saturation to occur), the water saturated slab was removed and weighed. It is known that the volume of the water absorbed by a porous sample (the slab) is equal to the volume of voids in the sample, if there are no closed pores and microcapillaries, (Hillel, 1980).

Hence,

$$V_a = \frac{M_\omega - M_s}{d_\omega} \qquad (4.4)$$

where , V_a is volume of water absorbed,

M_s is weight of oven dried slab,

M_ω is weight of water saturated slab,

d_ω is density of water.

Porosity which is defined as the percentage ratio of volume of air spaces (voids) to the bulk volume was calculated using the formula;

$$\rho = \frac{V_a}{V_b} \times 100\% \qquad (4.5)$$

where, V_b = volume of the sample slab.

4.6 Moisture content

Moisture content or water content is defined as the ratio of the mass of water in a sample to the mass of the sample after it has been dried to a constant mass at 105 °C. Moisture content is expressed as a percentage.

$$W = \frac{M_\omega - M_s}{M_s - M} \times 100\% \qquad (4.6)$$

where , M is mass of container in which sample is placed,

M_ω is mass of container with wet sample,

M_s is mass of container and oven dried sample.

It is possible to adjust the moisture content from a known initial value W_1 %, to a required value W %. (see appendix (1), Table 16).

In this work, mass of oven dried samples was obtained and their moisture contents varied by evenly sprinkling appropriate amount of distilled water to the samples. The samples were then left in a closed container to attain uniform moisture content. The above procedure of calculation of moisture content was then followed.

4.7 Measurement of temperature.

The sample holder with the samples was carefully placed in an oven. The temperature of the oven was increased at intervals of 50 °C from ambient temperature to 300 °C. Care was taken here to avoid the electrical leads from getting burnt. Asbestos coated leads were used in this case. Measurements of thermal conductivity with temperature were made as described in section 4.8 below.

4.8 Method of measurement of thermal conductivity

The Transient Hot-Strip method was used to measure thermal conductivity as described in chapter 3. The sample holder made of wood was designed such that there were two identical pieces of wood each of outer dimension 140 mm x 80 mm x 10 mm, containing rectangular troughs of dimension 71 mm x 41 mm x 5 mm, in which the sample slabs were laid.

Fig. 4.2 Typical experimental arrangement of the THS method.

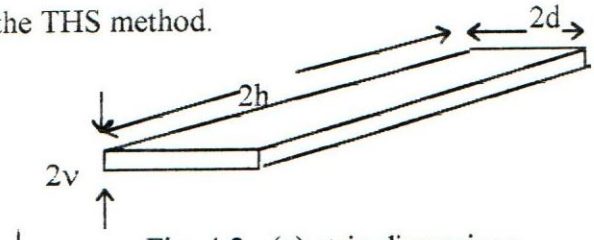


Fig. 4.2 (a) strip dimensions

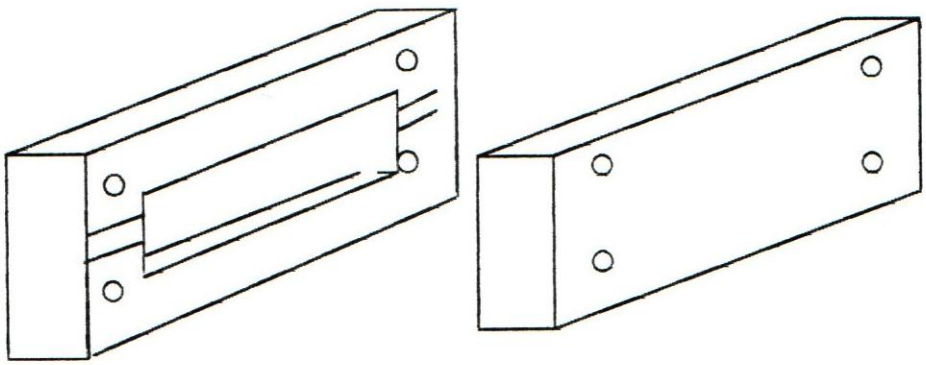


Fig. 4.2 (b) slab holders

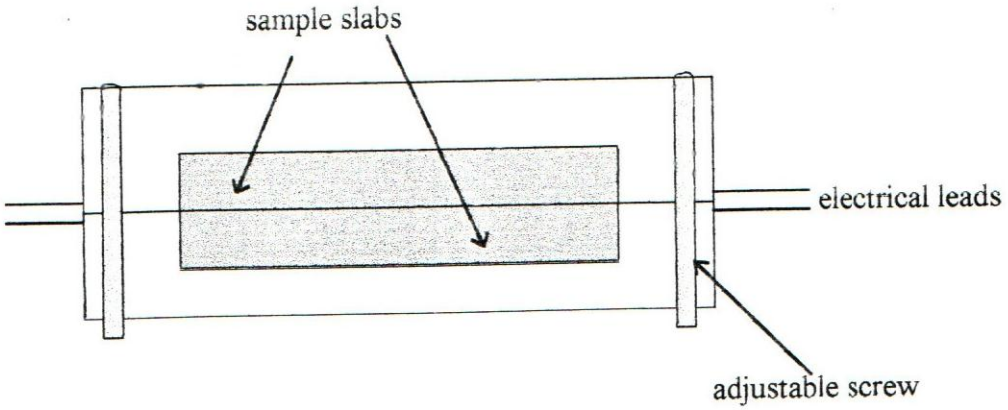


Fig. 4.2 (c) Clamping the strip between two identical slabs of the sample in the sample holder (Cross- section).

The sample holders were made with flat faces having surface areas large enough to be able to support a weight of about 15N so as to ensure good thermal contact and even distribution of applied force between the slabs and heating element. Two identical pieces of test specimen slabs made of the material to be investigated, of dimension 40 mm x 70 mm x 5 mm, were fixed in the sample holder with an aluminium strip i.e., the hot strip, (see Fig. 4.2 (a)) measuring 5 mm x 70 mm x 25 μm clamped between the two slabs.

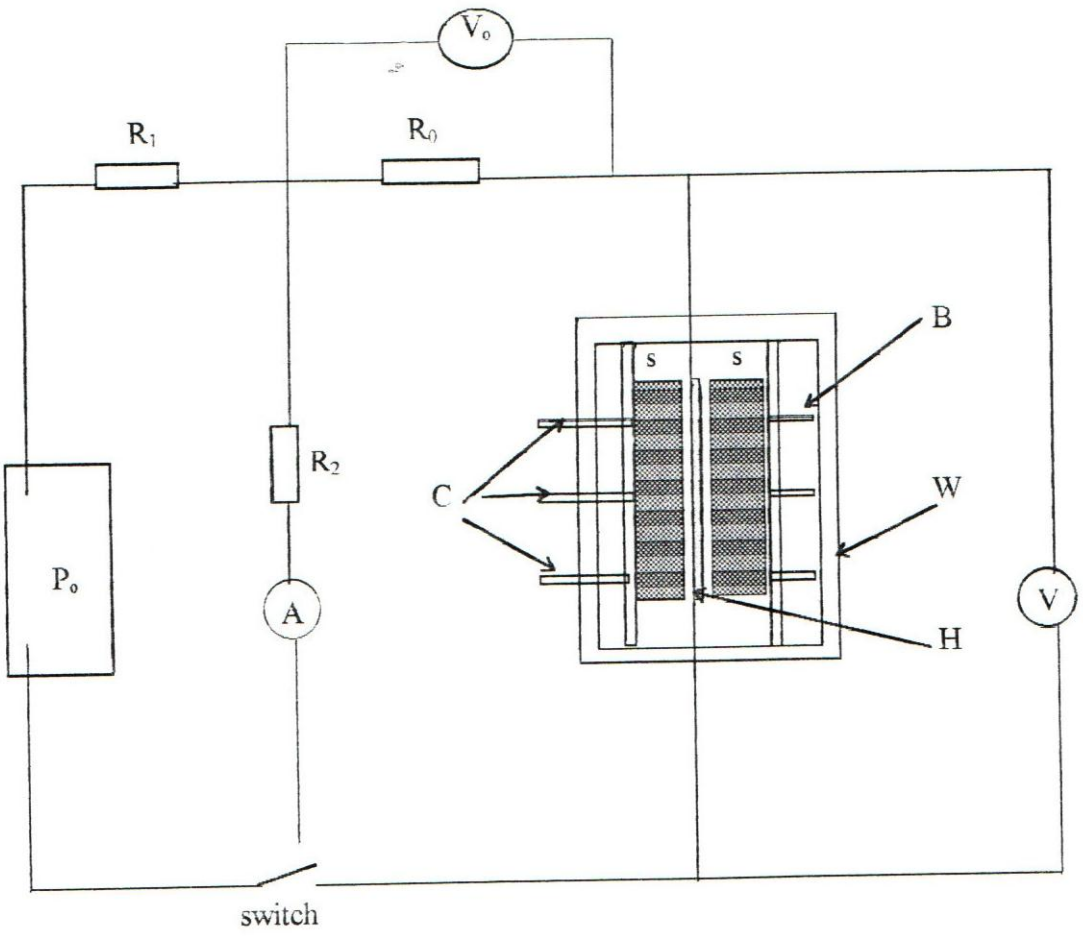
The choice of the strip dimensions is not arbitrary for measurement of thermal conductivities when using the THS method. The ratio of thickness to the width of the strip should be of the order of 10^{-3} (Log, 1992). This is in order to make the strip appear infinitely small compared to the test sample - one of the conditions of THS measurements. Consequently, a negligibly small fraction of heat is hindered by the air filled slots created at the edge of the strip when pressed between the slabs (Suleiman, 1994). The temperature coefficient of resistivity (TCR) of aluminium at room temperature is about 4.4×10^{-3} $^{o}C^{-1}$. Slots were made at the inner centre of the sample holders in order to accommodate the electrical leads.

The electrical circuit consisted of a constant voltage supply (Griffin regulated power supply, 800 mA continous load), and the heat source (temperature sensor) in series with time- independent standard resistor R_1 and current limiting resistor R_o. In most cases R_o has almost the same value as the initial resistance of the heat source. A balancing resistance R_2 was connected to ensure constant current flow for the duration of the experiment. The value of this constant current was measured by noting the reading of the ammeter A, and was maintained constant using a Rheostat. The increase in voltage across the heat source was recorded with a Fluke (8050 A) digital multimeter. This was done at a recording rate of 1 reading every 10 seconds.

For measurement and calculation of thermal conductivity, a constant current sufficient enough to cause some temperature increment was passed through the aluminium strip. Due to this temperature increment, the resistance of the strip changed and there was a corresponding change in voltage drop across the strip. By recording this voltage variation over a short time period from the onset of the heating current, it is possible to obtain precise information on the heat flow between the strip and the sample after a very short transient initial period (Log, 1992).

4.8.1 Experimental circuit

Fig. 4.3. Circuit diagram for measurement of thermal conductivity.



S is the sample, W is the wooden box (environment chamber),

H is the thin aluminium foil, B is the wooden baton, C are adjustable bolts,

P is the power supply, R_o is the standard resistor,

R_1 is the current limiting resistor, R_2 is the balancing resistor,

V_o and V are digital limiting voltmeters, A is the ammeter.

The voltage variation along the aluminium strip under the assumption of constant heat liberation from the strip is given by the formula, (Gustafsson et al, 1979; 1982);

$$V = V_0 + Cf(\gamma) \tag{4.7}$$

in which,

$$C = \frac{\alpha V_0 P_0}{4\pi^{1/2}\Lambda h} \tag{4.7.1}$$

where, α is the TCR for aluminium,

P_o is the total power output in the strip,

Λ is the thermal conductivity of the material surrounding the strip,

2h is the length of the strip,

V_o is the initial voltage across the strip before start of transient heating,

V is the voltage across the strip at transient time t.

CHAPTER 5

5.0 RESULTS AND DISCUSSION

5.1 Physical and mineralogical analysis of Wood ash and Diatomite.

Wood ash and Diatomite consist of the following compounds;

Table 5. Wood ash mineralogical composition (Average values):(Aduda, 1987; Erich and Ohno, 1992).

Compound	CaO	Al_2O_3	SiO_2	MgO	K_2O	Fe_2O_3	LOI
Quantity (%)	29.0	7.45	5.20	4.81	3.40	2.0	42.4

Table 6. Diatomite mineralogical composition (Average values): (African Diatomite industries, 1996; Mohsenin,

1980; Miranda et al, 1994).

Compound	SiO_2	Al_2O_3	K_2O	Fe_2O_3	CaO	LOI
Quantity (%)	86.90	3.32	2.58	1.28	0.48	5.45

It has been shown that for wood ash, loss on ignition is the most dominant, (42.4 %) (Aduda, 1987) meaning that there is a high percentage of water in the sample. The next abundant mineral is found to be Lime (CaO), 29.0 % , followed by Alumina (Al_2O_3), 7.45 %. The rest of the minerals as in the table above appear only in traces within the material. For diatomite it has been generally shown that Silica (SiO_2), loss on ignition and Alumina (Al_2O_3), are the most abundant with 86.90 %, 5.45 % and

3.32 % respectively. These are followed by Potash (K_20), 2.58 % and Ferric Oxide (Fe_2O_3), 1.28 %. Lime here is just a trace.

Physical description of the samples;

Table 7 Physical description of wood ash, F and Bu diatomite

SAMPLE	Wood ash	Bu- diatomite	F- diatomite
COLOUR	greyish	whitish	whitish brown
FEEL OF TOUCH	gritty	smooth and powdery	very smooth and powdery
WHEN MOIST	not sticky	sticky	sticky
PARTICLES IN WATER	particles settle fast	some particles settle slowly	particles remain suspended
CONSOLIDATED (SLAB) FORM	breaks easily	compact and does not break easily	very compact does not break

From this analysis, the various colours of the samples are due to the dominating constituents of the samples. In wood ash for example, the dominating minerals are Lime and Alumina, (Aduda, 1987; Erich and Ohno, 1992) which are generally whitish and brown respectively, but since wood ash is a residue of burnt materials which are black due to oxidation, the sample appears greyish. On one hand substances containing alumina (Al_2O_3) are known (Erich and Ohno, 1992), to have a high degree of crystallinity, while substances containing lime (CaO) are not very much crystalline, but are able to form aggregates of the grains.

High loss on ignition, about 42.4 % as reported by Aduda, (1987) indicates the presence of water in wood ash. When wood ash is dry, individual particles feel gritty when rubbed between fingers,

they are not sticky when moist, and they settle very fast to the bottom of a container of water because they are generally large and form aggregate of grains. Because of these factors wood ash portrays low compactibility. Crystallinity and formation of aggregates of grains would enable wood ash to be used as a refractory material capable of withstanding high temperatures without deformation.

Whitish and pale brown appearances of F and Bu diatomite respectively are due to the dominating minerals silica and alumina. Presence of silica indicates that the samples have high proportions of quartz, a mineral characterised by low porosity, (Uehara, 1981). Generally, diatomite has a comparatively low porosity. Due to the fineness of this mineral diatomite feels smooth and powdery to touch and its particles would be suspended in water for long. Alumina and Ferric oxide provide cementation providing a large shear strength (Miranda et al, 1994). The most probable reason why diatomite provides cementation and large shear strength could be due to high compactibillity and plasticity. Plasticity is the property of a material that enables it to change shape without producing surface cracks or rapture in its moulded state, (Ghildyal and Tripathi, 1987). Like clay, diatomite can be moulded into any shape upon application of a force that would make it exceed yield strength. The shape of the mould (slabs as in this study) formed remains unchanged even after water has been removed. Plasticity is the resultant effect of stress and deformation. Wood ash could be moulded when wet in its fine particle state, but disintegrates on drying, showing its non-plastic nature compared to diatomite.

5.2 Composition of composite mixtures of wood ash (WA) and diatomite (F and Bu types)

These consist of;

(a) three sample with particle sizes in the range 74-100 μm, and are shown in Tables 8 - 10.

Table 8. Thermal conductivities of composite mixtures of wood ash, F and Bu diatomite (wood ash constant)

composition by mass % WA	BU	F	Thermal conductivity x 10^{-2} (W m^{-1} K^{-1})
50	40	10	0.858
50	30	20	0.964
50	20	30	4.625
50	10	40	6.621

From Table 8, it is noted that as the F diatomite is increased and Bu diatomite decreased (WA constant), thermal conductivity appears to be increasing. Higher values of thermal conductivity are seen in the wood ash/ F diatomite mixture, while low values are noted for the mixture containing higher percentages by mass of wood ash and Bu diatomite (0.858 x 10^{-2} and 0.964 x 10^{-2} W m^{-1} K^{-1}).

Table 9. Thermal conductivities of composite mixtures of wood ash, F and Bu diatomite, (F diatomite constant

composition by mass % F	WA	BU	Thermal conductivity x 10^{-2} (W m^{-1} K^{-1})
50	40	10	0.987
50	30	20	1.577
50	20	30	6.796
50	10	40	3.0224

From Table 9, thermal conductivity appears to increase as the wood ash content in the mixtures is decreased and as the Bu diatomite content is increased, except for the 50 %/ 10 %/40 %, F/ WA/ Bu composite. High values of thermal conductivity are observed in the composite having high percentages by mass of Bu and F diatomite mixtures. Low values are observed in the mixture having high percentage by mass of F diatomite and low percentage by mass of wood ash. The highest value of thermal conductivity i.e., 6.796 x 10^{-2} W m^{-1} K^{-1}, appears for the mixture of 50 % F diatomite, 20 % wood ash and 30 % Bu diatomite. This abnormally high value could be explained by the enhanced thermal contact between particles as the percentage of both Bu and F diatomite increases.

Table 10. Thermal conductivities of composite mixtures of wood ash, F and Bu diatomite (Bu diatomite constant

composition by mass %			Thermal conductivity
BU	F	WA	x 10^{-2} (W m^{-1} K^{-1})
50	40	10	3.859
50	30	20	3.090
50	20	30	5.691
50	10	40	1.1976

In this case thermal conductivity appears to decrease as the percentage by mass of wood ash increases and that of F diatomite decreases. As in Table 9 above, high values of thermal conductivity are observed in the mixtures having high percentages by mass of F and Bu diatomite, except for the mixture containing 50 % Bu diatomite, 20 %, F diatomite and 30 % wood ash. The value here is 5.691 x 10^{-2} W m^{-1} K^{-1}, which may have arisen due to a minimum number of voids in this mixture. The little voids present could also have contributed to this value of thermal conductivity in this composite as a

result of radiative heat transfer (Kanan et al, 1989). However, a low thermal conductivity value is observed in the composite having high percentages of wood ash and Bu diatomite. This is in agreement with the trend in Table 8 above.

(b) two samples with particle sizes in the range 74 - 100 μm as shown in Tables 11 - 13.

Table 11. Thermal conductivities of composite mixtures of F and Bu diatomite

composition by mass %		Thermal conductivity
Bu	F	x 10^{-2} (W m^{-1} K^{-1})
75	25	4.955
50	50	0.623
25	75	1.1908

There are high values of thermal conductivity in the composite containing high percentages of both samples, but a low value is seen in the 50 % - 50 % mixture. This is because of non- enhanced particle- particle contact, no sample is in excess and particle size distribution is uniform.

Table 12. Thermal conductivities of WA and F diatomite composite mixtures

composition by mass %		Thermal conductivity
WA	F	x 10^{-2} (W m^{-1} K^{-1})
75	25	0.0590
50	50	1.798
25	75	1.929

As the percentage of F diatomite is increased and that of wood ash is decreased thermal conductivity increases. It if F diatomite that dominates in which we know that particles are more close together and therefore have better heat conduction.

Table 13. Thermal conductivities of wood ash and Bu composite mixtures

composition by mass %		Thermal conductivity
WA	Bu	x 10^{-2} (W m^{-1} K^{-1})
75	25	0.0126
50	50	0.0154
25	75	0.987

In table 13, thermal conductivity values are increasing as the percentage of Bu diatomite is increased and as that of wood ash is decreased. In these composites (Table 13) values of thermal conductivity are rather low compared to those shown in Tables 11 and 12.

From Figures 5.1 and 5.2, it is evident that those composites having high percentage by mass of both wood ash and F diatomite as well as those having high percentage by mass of Bu and F diatomite have the highest values of thermal conductivity. This could be explained by the nature of the individual particles. Particles of F diatomite which is more powdery of the three, interlock with those of wood ash and Bu diatomite thus bridging the gap between individual particles. This improves the thermal contact making the thermal conductivity high (Luikov, 1964).

There is a rather low particle- particle interaction in the composite having a high percentage by mass of wood ash and Bu diatomite mixture. The air within the pores of this mixture is responsible for the low values of thermal conductivity (Luikov et al, 1966). It is therefore expected that the best

thermal insulators could come from the composite with high percentages of wood ash and Bu diatomite. This agrees well with the low values of thermal conductivity for wood ash and Bu diatomite as shown in figure 5.4.

Fig. 5.1 Variation of thermal conductivity with percentage composition by mass of composite mixtures comprising 3 samples.

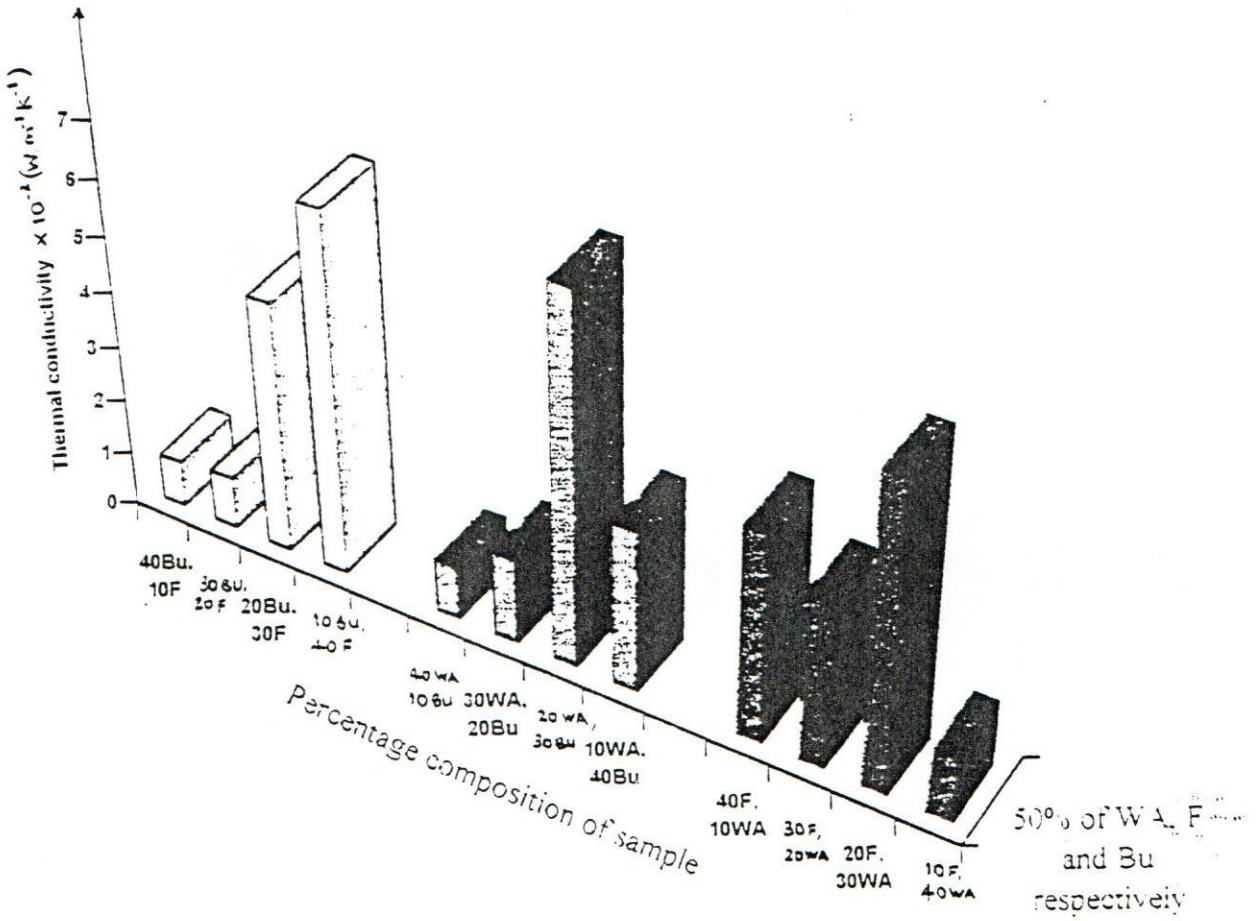
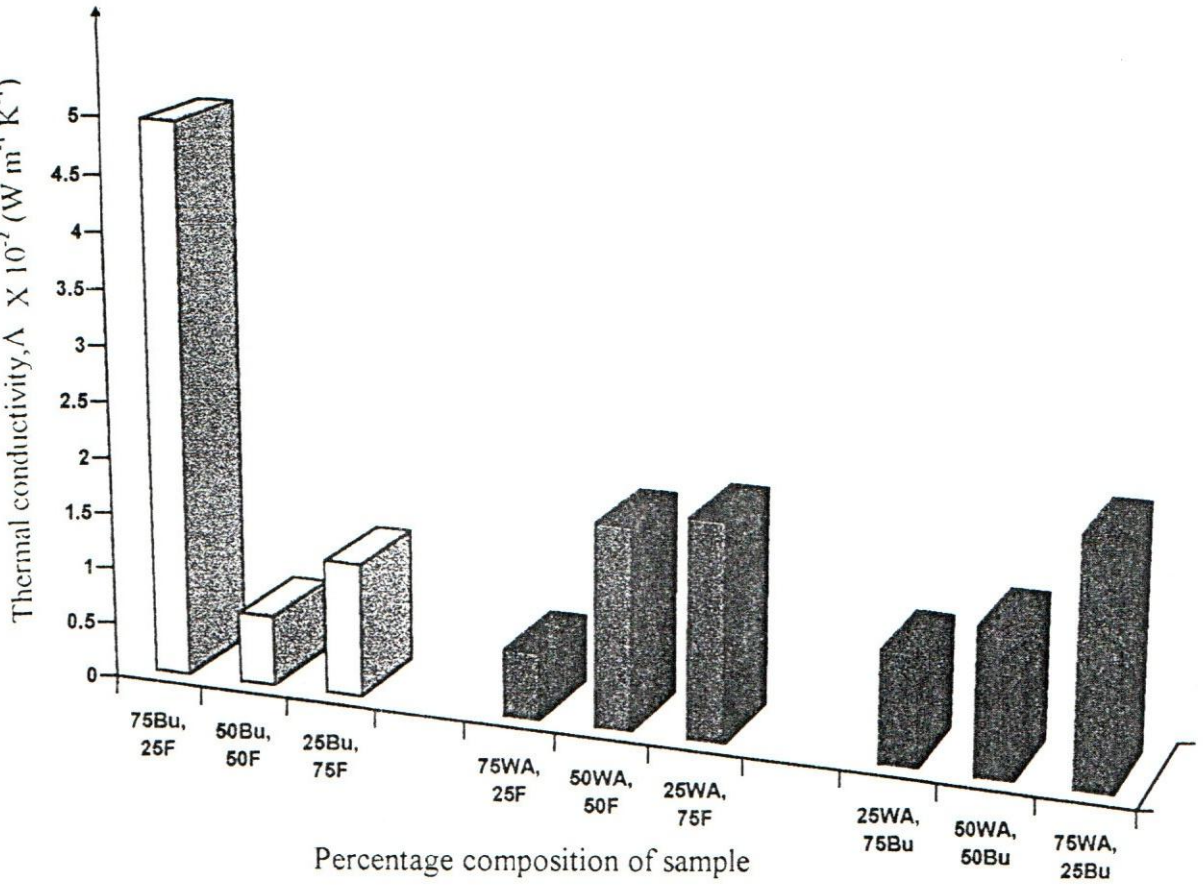


Fig. 5.2 Variation of thermal conductivity with percentage composition by mass of composite mixtures comprising 2 samples.



Comparing Figures 5.1 and 5.2, it is seen generally that absence of any one sample in the composite mixtures to some extent influences the values of thermal conductivity. In Fig. 5.1 the composites with 50 % wood ash show lower values of thermal conductivity than those having 0 % wood ash in Fig. 5.2. Composites having 50 % F diatomite but varying composition of wood ash and Bu diatomite display higher values of thermal conductivity than those having 0 % F diatomite. Composites having 50 % Bu diatomite have slightly higher values of thermal conductivity than those with 0 % Bu diatomite. From this comparison, it can be concluded that thermal conductivity in any composite mixture will decrease as the amount of wood ash is increased, while it increases as the amount of F diatomite is increased. We have moderate values of thermal conductivity in composites having Bu diatomite and as it is increased as shown by Tables 8, 9, 11 and 13.

5.3 Particle size distribution analysis

For the purpose of preparation of the specimen into correct particle sizes, the samples were conveniently grouped into various particle sizes, Table 14. These were then classified in terms of percentage by dry weights of the samples retained by the sieves during the sieving process, Table 15.

Table 14. Sample particle size distribution

Sample group	Particle size (diameter range in μm)
Coarse grained	1000 - 500
Medium grained	500 - 100
Fine grained	100 and below

Table 15. Percentage by dry weight of wood ash (WA), F and Bu diatomite retained by respective sieve sizes.

Particle size (μm) (App. diameter range)	% by weight of sample retained		
	WA	F	Bu
> 1000	10.08	5.71	6.64
1000- 500	19.22	6.20	30.79
500 - 100	33.73	16.68	36.38
100 - 74	24.85	34.04	21.23
74 - 45	9.87	32.30	4.17
45 - 0	2.25	4.97	0.80

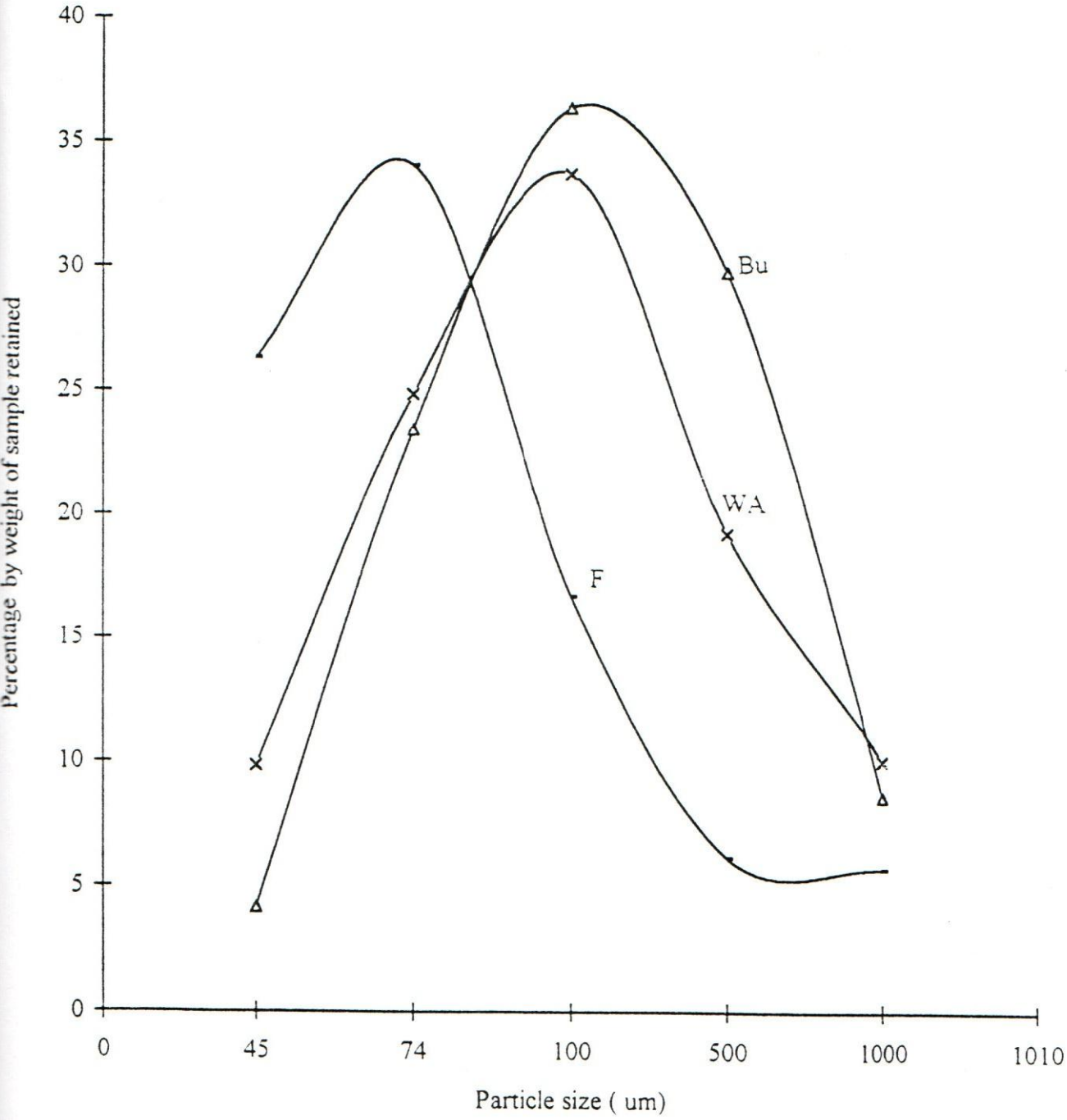
It was noted that however much the amount of the sample placed on the sieves, equal percentages of sample were retained or passed through in equal time intervals. Out of the three samples used, F diatomite is the most well graded, as can be seen from the smooth curve F in figure 5.3. It is followed by wood ash then F diatomite.

The distribution curves also show large percentages (> 35 %), of particles of size greater than about 100 μm for the Bu diatomite. As compared to WA and Bu samples, most of the F diatomite lie in the fine particle diameter range (Table 14). This agrees well with data in Table 7, that F diatomite is powdery and smooth to touch. F diatomite will make slabs (moulds) that are compact and do not break easily. This is duet to the high plasticity of F diatomite in comparison with wood ash and Bu diatomite. It is also expected that in their moulded states, wood ash is more brittle since plasticity is low and there is limited close packing of the particles. The distribution of wood ash is such that there is a small percentage (< 30 %), of grains in the fine particle range. The graphs also show a coincidence for all the samples of grain size 79 μm. They all have a percentage by weight of 29.30 % of the particles retained. It is important to note that it is from this group of particle size range (79- 100 μm) that thermal conductivity was determined against all other factors in this study.

These curves (Fig. 5.3) show a similar trend with the studies on two types of clays; Red and Black (Kinyanjui, 1995) and on copper powders (Bala et al, 1989). The adsorptive capacity of a porous material is determined by its specific surface area, which is directly proportional to the porosity and inversely proportional to the pore size (Lyall, 1972). We note that those samples with low porosity consequently have smaller pore size. These samples in the fine and the medium grained category could very well serve as fluid absorbents (African Diatomite Industries, 1996). It is also noted that the fine grained samples have smaller pores and therefore have greater interconnection by means of

fine channels, a factor that contributes highly to adsorption. However the rate of adsorption will depend also on the number of pores facing the source of the medium being adsorbed. The greater the number of pores, the greater the adsorbing area of the material (Lyall, 1972; Odhiambo, 1969).

Fig. 5.3 Percentage by weight of particle size distributions for wood ash, F and Bu diatomite



5.3.1 Thermal conductivity and particle size

The three curves in Figure 5.4 display a similar trend. In the lower particle size range, (0- 45 μm) all the samples have high values of thermal conductivity. This is followed by a sharp decrease in thermal conductivity which reaches 1.56 x 10^{-3} W m^{-1} K^{-1} at particle size 45 μm for Bu diatomite, 2.45 x 10^{-3} W m^{-1} K^{-1} for F diatomite and 2.89 x 10^{-3} W m^{-1} K^{-1} for wood ash, both at particle size 74 μm. For F and WA, there is a gradual decrease in thermal conductivity as particle sizes increase from 12.5 to 74 μm. A sharp increase is then noted as the particle sizes increase from 74 to 100 μm. A. These comparatively high values of thermal conductivity show that there is a better particle- particle contact in F diatomite as seen in section 5.2 of this work. For Bu diatomite, there is a decrease in thermal conductivity from 12.5 to 45 μm, then a gradual rise in the higher particle size range. In general, the curves show that there are low values of thermal conductivity for both WA and Bu diatomite.

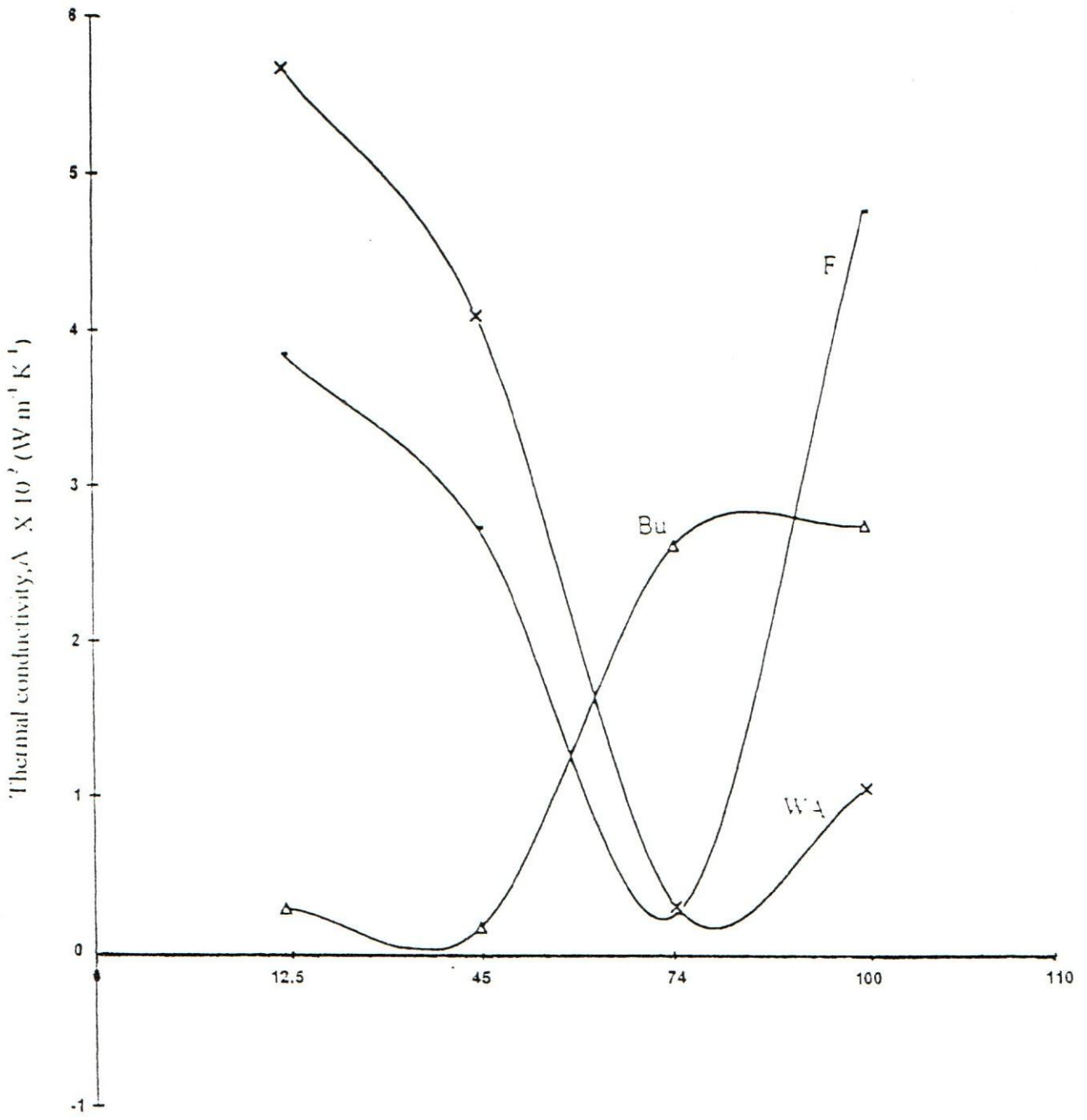
However at lower particle size range, wood ash is seen to have higher values of thermal conductivity than both Bu and f diatomite. This can be attributed to the somewhat low porosity at the low particle size range. At low porosity (20 %- 40 %) there is a high concentration of the solid phase, which is known to have the highest thermal conductivity than any other phase, (Kinyanjui, 1995). In the larger particle size range 74- 100 μm, wood ash has very low thermal conductivity. This is due to decreased solid phase concentration.

It is obvious that thermal conductivity of granular systems in various particle sizes will depend upon the intimacy of the contact of solid particles, the grain shape, the spaces between projections of roughness of the contact surfaces and presence of pores within the grains. From a single contact surface, we get heat flow through direct conduction from grain to grain. There is also conduction

through the medium (air) filling the pores and the spaces between the projection of roughness (orientation) of the grains, radiative heat between surface and gas convection in the pores (Luikov et al, 1966).

Thermal conductivity is decreasing in the lower particle size range, because of an excess thermal resistance created within the region of immediate proximity of contact, since the contact surface of any two particles represents additional resistance to heat exchange between particles (Touloukian, 1970). At about 100 μm the grain shapes and contact improve and direct conduction through contact is enhanced, hence thermal conductivity increases. At higher particle sizes air filling the pores between the grains circulates through the solid. Air has lower thermal conductivity than the solid phase (Luikov, 1964), and it is because of this that we have a gradual decrease in thermal conductivity in this range.

Fig. 5 4 Variation of thermal conductivity with particle size for wood ash, F and Bu diatomite

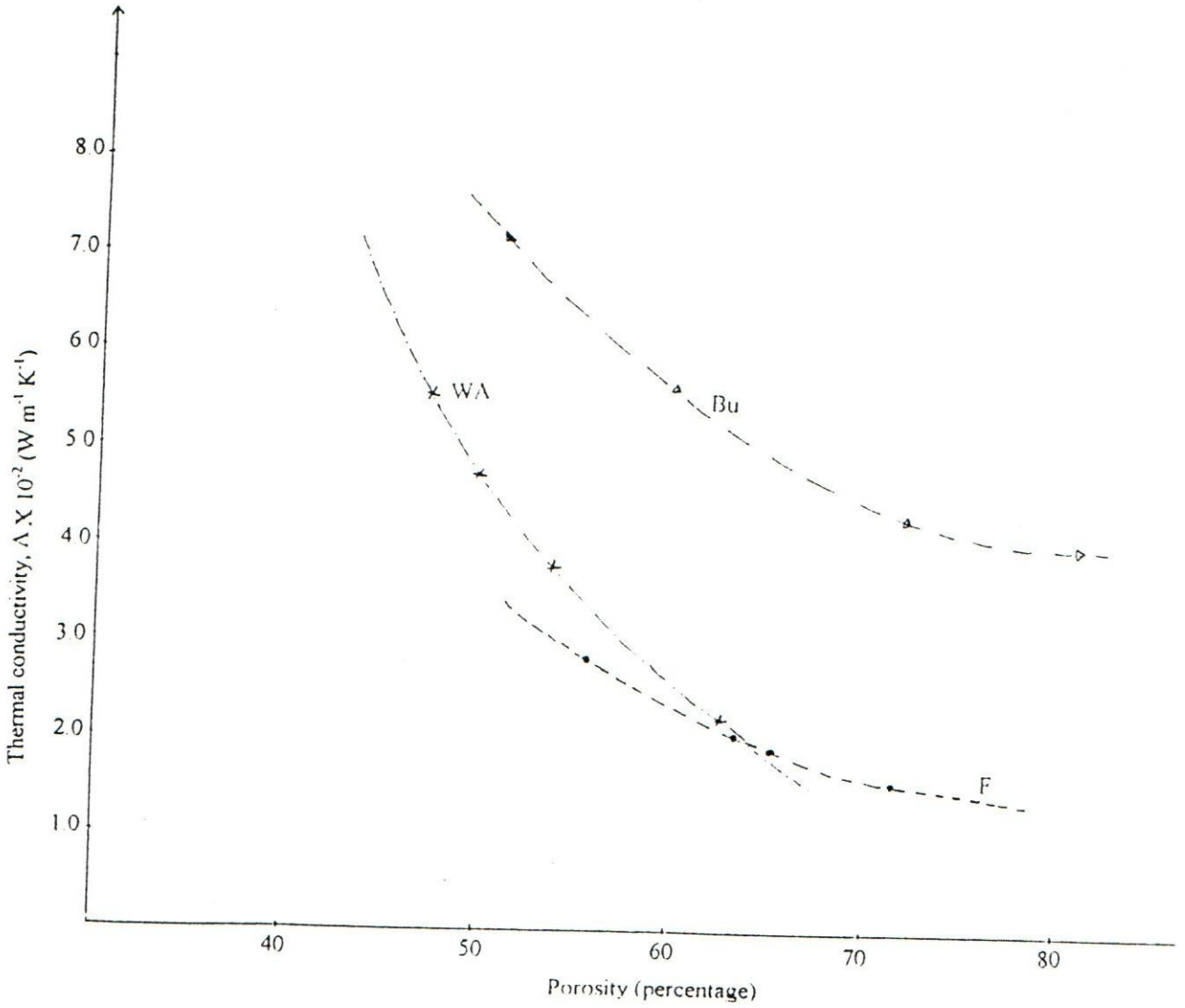


5.4 Thermal conductivity and porosity

Variations of thermal conductivity with porosity of wood ash, F and Bu diatomite (Figure 5.5), show that for very low porosities, thermal conductivity values are high, i.e., between 2.85 x 10^{-2} and 7.25 x 10^{-2} W m^{-1} K^{-1} as expected. As porosity increases there is remarkable decrease in thermal conductivity. These trends are in good agreement with those of Woodside and Messmer, (1961), Figure 2.2 and Wimmer's model (Kanan et al, 1989), Figure 3.6.

In this study values of thermal conductivity are high for Bu diatomite, ranging from 7.25 x 10^{-2} W m^{-1} K^{-1} at 51.07 % porosity down to 4.00 x 10^{-2} W m^{-1} K^{-1} at 80.59 % porosity. This is followed by wood ash from 5.61 x 10^{-2} W m^{-1} K^{-1} at a low porosity of 47.50 % to 2.252 x 10^{-2} W m^{-1} K^{-1} at 62.5 % porosity. Finally there is F diatomite with 2.85 x 10^{-2} W m^{-1} K^{-1} at 56.38 % porosity to 1.59 x 10^{-2} W m^{-1} K^{-1} at 71.74 % porosity. At low porosity the high values of thermal conductivity can be explained by the fact that there is increased contact thermal conductivity, (Luikov et al, 1966), all measurements done at room temperature. In comparison with the graphs of Woodside and Messmer (1956) (Figure 2.2), for variation of thermal conductivity with porosity of water saturated sandstones, the differences could be due to the different saturants within the pores. Water as a saturant has a very high conductivity compared to air, hence it is expected that the water saturated sandstones in the Woodside and Messmer study, will have higher values of thermal conductivity as opposed to air filled samples of diatomite and wood ash.

Fig. 5.5 Variation of thermal conductivity with porosity for wood ash, Bu and F diatomite



5.5 Variation of thermal conductivity with moisture content

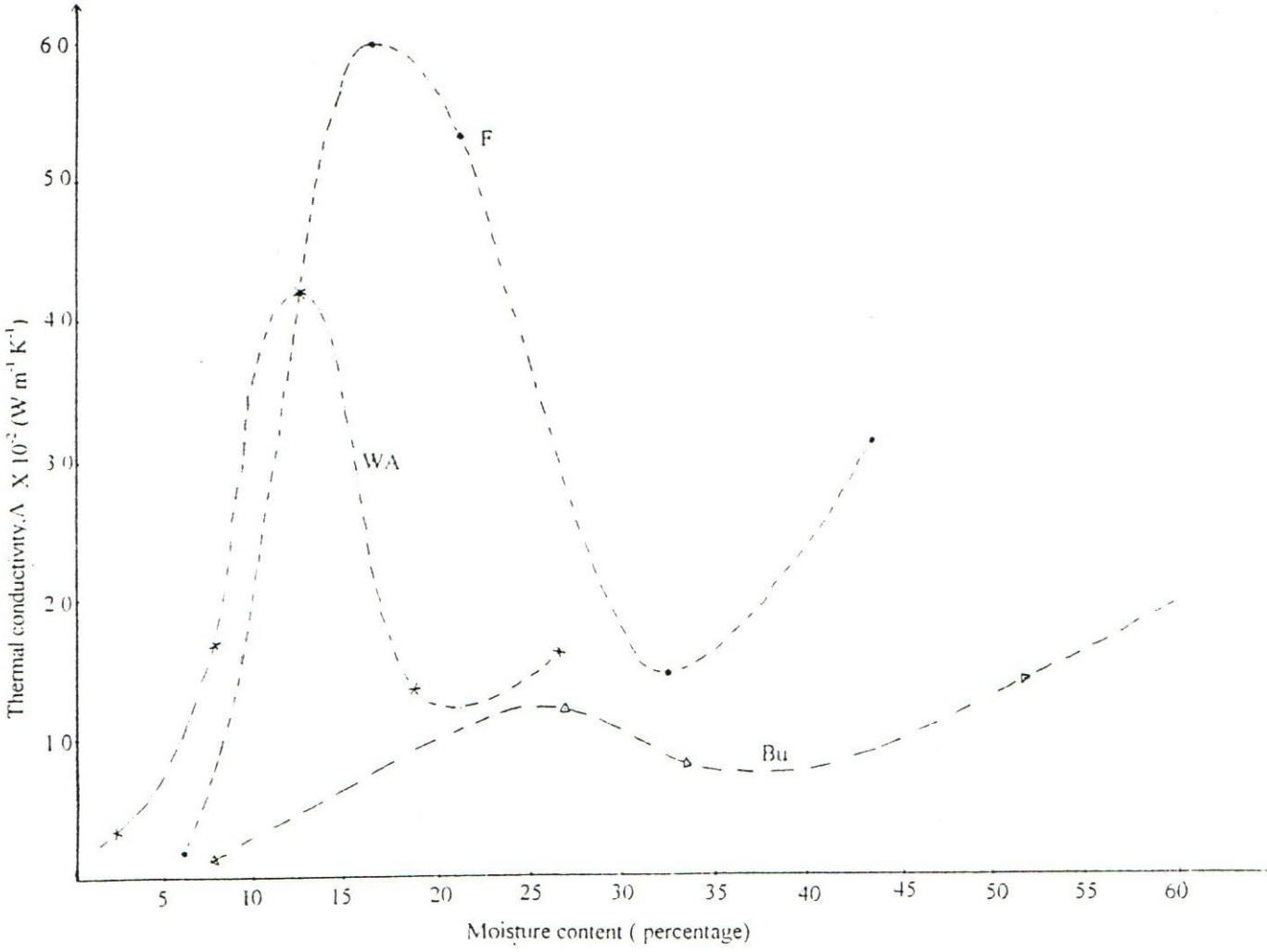
There is generally a similar trend for all the samples used in this study (Fig. 5.6). It is seen that there is a gradual increase in thermal conductivity with moisture contents between 0 % and 10 % for WA, between 6 % and 17 % for F diatomite and between 7 % and 26 % for Bu . This is followed by a rapid decrease in thermal conductivity for moisture content between 10 % and 18 % in wood ash, between 17 % and 33 % in F diatomite and between 26 % and 34 % in Bu diatomite. Then there is an increase above 20 % for WA, above 33 % for F diatomite and above 39 % water content for Bu diatomite. In general the highest values for thermal conductivity are those for F diatomite, followed by wood ash then Bu diatomite.

For low moisture content, increase in thermal conductivity values can probably be attributed to the presence of a relatively thin film of water on the surface of particles as compared to a large volume of void filled with air. Since air is a relatively poor conductor of heat compared to water, there is poor thermal contact between solid particles hence a low value of thermal conductivity (Luikov, 1964). As moisture content is increased, thermal contact increases since water has a thermal conductivity about 23 times higher than air, (Ghildyal and Tripathi, 1978). Thermal conductivity therefore increases.

At mid moisture contents (10 % - 20 % for WA and 17% - 26 % for Bu and F diatomite), there is a decrease in thermal conductivity. When there is sufficient moisture in a sample, the orientation of particles and their subsequent sliding over each other will take place in order to create a film around each particle. At these moisture content the particles are randomly oriented meaning that there are low interactions and low thermal contact, hence the decrease in thermal conductivity. When moisture content increases for the particles to reach the lower plastic limit, the particles get reoriented and there is improved contact (Ghildyal and Tripathi, 1978; Hillel, 1980). Thermal conductivity is seen to increase with moisture content

above 20 % for WA and above 30 % for F and Bu diatomite. The film tension holds the particles together and the particles will slide over each other.

Fig. 5.6 Variation of thermal conductivity with moisture content for wood ash, Bu and F diatomite



At very high water contents, hydrogen bonding in the water causes an orientation of water molecules on the solid particles (Ghildyal and Tripathi, 1978). The thickness of water layer is now high. Plasticity of the sample is also high, but the factor that contributes to a sudden drop in thermal conductivity at this stage could be the included water vapour movement (heat from the heat source), in the solid- liquid interphase. This vapour movement reduces the transfer of heat resulting in low values of thermal conductivity (Oswal, 1983).

At even higher moisture contents, thermal conductivity increases steadily for each of the samples a results of excess water and the effective thermal conductivity is that of water and solid particles combined.

Despite the similarities in variation of thermal conductivity with moisture content for wood ash, F and Bu diatomite, there are different values for thermal conductivities for the same moisture contents. These differences are the results of different compaction of particles and bulk density (Oswal, 1983).

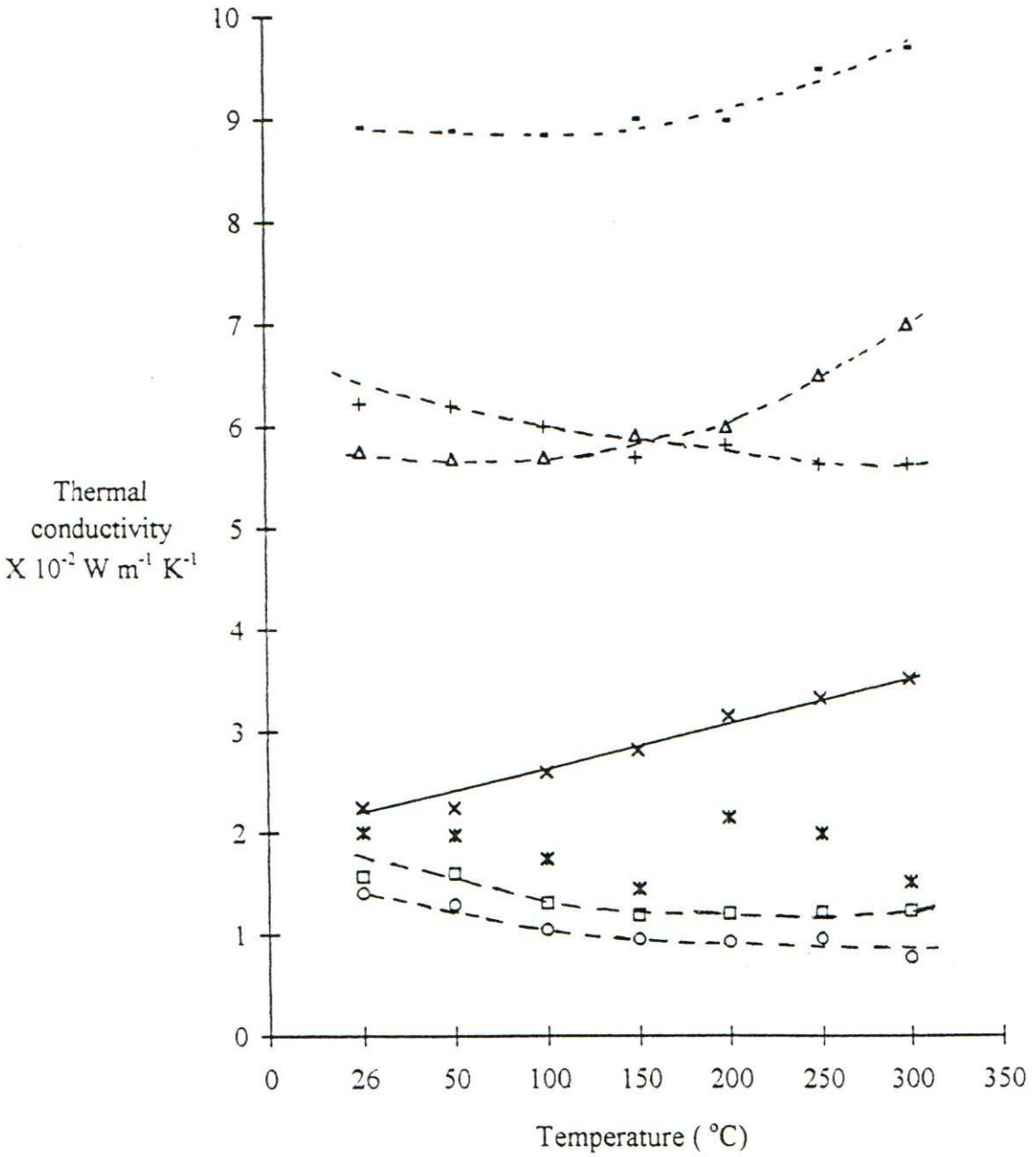
5.6 Variation of thermal conductivity with temperature

It is noted that thermal conductivities for 'pure' wood ash, F and Bu diatomite generally increase as the temperature is increased from room temperature, 26 °C, to 300 °C as can be seen in Fig. 5.7. There are high values of thermal conductivity for F diatomite, between 8.92×10^{-2} W m^{-1} K^{-1} and 9.70×10^{-2} W m^{-1} K^{-1} within this range of temperature. The next highest is Bu diatomite with values of thermal conductivity between 5.75×10^{-2} W m^{-1} K^{-1} and 7.00×10^{-2} W m^{-1} K^{-1}. We have the lowest values in wood ash, between 2.25×10^{-2} W m^{-1} K^{-1} and 3.51×10^{-2} W m^{-1} K^{-1}. Despite the porosities for the three being somewhat similar i.e., F diatomite- 63.13 %, Bu diatomite- 60.12 % and wood ash- 62.50 %, there is variation in the thermal conductivities, which can be explained by conduction of heat in the pores coupled with radiative heat transfer which increases as the pore size increases, and it plays an increasingly active role at high temperatures (Touloukian, 1970).

The relatively high thermal conductivities for F diatomite can be attributed to small pores which increase the heat transfer. Pore size is therefore an important microstructural feature. For optimum thermal resistance, it is desirable to have the pore size small and the pore phase continuous (Pratt, 1969). The upward facing curves indicate a strong influence of conduction through the air spaces. At high temperatures, radiative heat transfer takes place through the fluid phase of the samples (Aduda, 1996). Comparing wood ash and diatomite in the same porosity and particle size, diatomite samples have higher values of thermal conductivities. This is the role played by the contact resistance as a result of arrangement and orientation at the particle- particle contact points. Low values of thermal conductivity seen in the composites of wood ash and diatomite are caused by the inhomogeneities at the particle-particle contact point. Inhomogeneities will greatly affect the conductivity resistance but not the total porosity, (Aduda, 1996; Luikov et al, 1966). For a given material there is a strong dependence ot

thermal conductivity with bulk density. The low value of thermal conductivity is due to air (a poor conductor) contained in the pores, rather than the thermal conductivity of solid particles alone. Variations of thermal conductivity in some materials e.g., composite mixtures depend on; (i) whether or not a crystalline structure is formed (Luikov, 1964), (ii) apparent bulk density of the material. These are reasons why thermal conductivity is seen to decrease as temperature increases (Fig. 5.7)

Fig. 5.7 Variation of thermal conductivity with temperature for samples of wood ash, Bu and F diatomite and their composites



- = F diatomite; Δ = Bu diatomite; x = Wood ash; + = F and Bu diatomite composite;

* = Wood ash, F and Bu diatomite composite; □ = Wood ash and F diatomite composite;

o = Wood ash and Bu diatomite composite

CHAPTER 6

6.0 CONCLUSIONS AND RECOMMENDATIONS

6.1 Conclusions

This study has found out that when considering porous materials (in the class of diatomite and wood ash), account must be taken of the fact that the particular properties of the actual grains of which the material is composed will determine the general nature and application of the material. The pores vary in size and shape and are randomly distributed. Those that are sufficiently small exclude convective and radiative heat transfers. It is mainly conductive heat transfer that takes place in this case. For more granular porous materials, there is a tendency of the pore sizes being large hence radiative heat transfer dominates especially at higher temperatures (above 250 °C) .

Specific surface area of a material is directly proportional to the porosity and inversely proportional to the pore size. Materials with very small and very large particle sizes have low porosity. Therefore high porosity materials have smaller pore size and greater interconnection by means of fine channels, and are therefore good adsorbents. Materials with low porosity on the other hand are good liquid filter aids.

Generally high lime and alumina content in wood ash provide crystallinity and low compactibillity. Wood ash is therefore capable of making good refractory material that can withstand high temperatures without deformation. Silica content in diatomite is characteristic of low porosity and this enables it to be used mainly as a filter aid. A combination of alumina and Ferric oxide content in wood ash/ diatomite composite provides cementation of particles. They can be moulded into any shape upon application of a force that exceeds their yield strengths.

Variation of thermal conductivities with particle size and porosity for wood ash and diatomite are in agreement with the results of Wimmer's model (Kanan, 1989). Thermal conductivity decreases as porosity is increased mainly due to increased voids in the samples allowing circulation of air (a poor insulator) between the particles. Since large voids inhibit heat conduction, high porosity samples of wood ash and diatomite can best be used as thermal insulators. Composite mixtures of these materials exhibit thermal insulator properties especially at high temperatures above 200 °C. Thermal conductivities of these composites decrease with increase in temperature. The nature of the grains and the heat paths along the grains also contribute to a material as an insulator.

Low values of thermal conductivity are noted in composite mixtures of wood ash and Bu diatomite, and those of wood ash and F diatomite in the range of temperature from about 30 °C to 300 °C. From the curves of variation of thermal conductivity with moisture content, thermal conductivity generally increases with moisture content, except for the range between 15 % and about 30 % moisture content. This is because of low thermal contact as a result of random orientation of particles, especially those of the composite mixtures comprising all the three samples.

Finally the experimentation agrees with the theory of thermal probe method of measurement of thermal conductivity which is the base for the THS method.

6.2 Recommendations

A few possibilities for further research, that were however not possible to attain here due to time limitation, may be mentioned;

(1). It is necessary to know the behaviour of wood ash and diatomite as thermal insulators at temperatures higher than 300 °C. There is a possibility that these materials can be used in high

temperature insulation. At these temperatures investigations of thermal diffusivity and specific heat can be made to establish the optimum temperature required before thermal stress occurs.

(2). Using the same set up of the THS method it is possible to measure the temperature coefficient of temperature (α) as well as the electrical resistivity of any hot-strip. However, this is only possible if the thermal conductivity of the porous sample is initially known.

REFERENCES

Aduda B. O. C (1987); *Thermal conductivity of porous insulators: Wood ash and Vermiculite.* MSc Thesis, University of Nairobi.

Aduda B. O. (1996); Effective thermal conductivity of loose particulate systems. J. Mat. Sci., 31; 6441- 6448.

African Diatomite Industries (1996); Private communication.

Arora C. P. (1989); *Heat and Mass Transfer*. Khanna, New Delhi; 3- 8

Allen T. (1990); *Particle size measurement.* Chapman and Hall 4th ed.; 192-371.

Baver L. D., W. H. Gardner, W. R. Gardner.(1972); *Soil Physics.* 4th ed.; John Wiley and sons, New York; 266-281.

Berman R. (1976); *Thermal conduction in solids.* 1st ed.; Clarendon Press, Oxford; 1- 178.

Bever M. B. (1986); *Encyclopedia of material science and Engineering.* Pergamon Press, New York, Vol. 5; 3566- 3572.

Black C. A., D. D. Evans, J. L. White, L. E. Ensminger, F. E. Clark. (1965); *Methods of soil analysis,* J. Am. Soc. of Agr. USA, 9: 25- 106.

Bragg (1948); *Science*. McGraw-Hill, New York, 108:455

Carslaw H. S. and J. C. Jaegar.(1959); *Conduction of heat in solids.* Oxford University Press, New York, 2: 339-341.

Chapman A. J. (1990); *Heat transfer.* Macmillan, 4: 20-27.

Chaudhary D. R. and R. C. Bhandari (1976); Thermal conductivity of two phase porous materials: dry soils. Brit. J. Appl. Phys. D, ser. 2 vol. 2, 609-610.

Clark F. E. (1940); *Applied X-rays*. McGraw Hill New York, 507.

Cornish E. H. (1987); *Materials and Design.* Cambridge University Press, UK. 1st ed.

Cornwell K. (1977); *The flow of heat.* Van Nostrand, New York, 1st ed.

Dunlap R. A. (1988); *Experimental Physics ; Modern methods.* Oxford University Press; 324-337.

Erich M. S. and T. Ohno (1992); Titrimetric Determination of Calcium-Carbonate Equivalence Of Wood Ash.. Analyst, Vol. 117. Iss. 6; 886- 995.

Finn C. B. P. (1993); *Thermal Physics.* Chapman and Hall, London 2 nd ed.; 32- 69.

Fountain J. A. and E. A. West (1970); J. Geophysics Research, 75 ,20: 63.

Garret K. W. and H. M. Rosenberg (1974); Thermal conductivity of epoxy-resin/powder composite metals. J. Phys. D, 7 ; 1247-1258.

Gerald F., M. Patricia, T. Lloyd, (1984); *Stoves and trees.* International Institute for Environment and Development, Russel, Washington; 32- 36.

Ghildyal B. P. and R. P. Tripathi, (1987); *Soil Physics.* Wiley Eastern Ltd. New Delhi 1st ed.

Gustafsson S. E. (1991); Transient plane source techniques for thermal conductivity and thermal measurements of solid materials. Rev. Sci. Instrum. 62(3); 797-804.

Gustafsson S. E., E. Karawaki and M. A. Chohan, (1986); Thermal transport studies of electrical conducting materials using the transient hot- strip technique. J. Phys. D: Appl. Phys. 19; 727- 735.

Gustafsson S. E. and E. Karawaki, (1985); Circuit design of transient measurements of electrical properties of thin metal films and thermal properties of insulating solids and liquids. Rev. Sci. Instrum. 55 (4); 610- 613.

Gustafsson S. E., E. Karawacki, N. M. Khan (1979); Transient hot-strip method of simultaneously measuring thermal conductivity and thermal diffusivity of solids and fluids. J. Phys. D: Appl. Phys. vol. 12; 1411-1421.

Head K. H. (1989); *Soil Technicians' Hand book.* Pentech Press, London, 1st ed.; 13.

Helsdon R. M. (1965); *Introduction to applied thermodynamics*, Pergamon Press, Oxford, 1st ed.; 59- 64.

Hey A. W. and Livey D. T. (1969), Calcination processes in oxides. Proc. Br. Ceram. Soc. 12; 13- 31.

Helmut K. (1968); *Soil colour.* 2nd ed.; 192- 200.

Helte A. (1993); Radiative and conductive heat transfer in porous media-estimation of the effective thermal conductivity. J. Appl. Phys. Vol. 73, Iss 11; 7167- 7173.

Hillel D. (1980); *Introduction to soil Physics.* Academic Press, 1st ed.; 26- 35.

Holmes J. W., and T. J. Marshall (1988); *Soil Physics*. Cambridge University Press, London. 2nd ed.

Jackson L. M. (1979); *Soil Chemical analysis; Advanced course*. A manual of methods useful for instructions and research in soil Chemistry, Physical Chemistry of soils, soil fertility and soil genesis, Published in U.S.A, 2nd ed.

Jaganmohan A. and S. P. Sukhatme (1968); *A transient method for determination of thermal conductivity and heat capacity of slab insulation*. 4HMT 68; 643-651.

Kanan B., R. P. Pradeep, N. S. Saxena and M. P. Saksena (1989); Effective thermal conductivity of Copper powders. J. Phys. D: Appl. Phys. 22; 1068- 1073.

Kinyanjui R. K. (1995); Thermal conductivity of unfired clays: Black and Red. MSc. Thesis, Egerton University.

Kimani J. N. (1989); Thermal conductivity of refractory brick materials. MSc. Thesis University of Nairobi.

Log T. (1993); Transient one- dimensional heat flow technique for measuring thermal conductivity of solids. Rev. Sci. Instrum. 64 (7); 1956- 1960.

Log T. (1992); Thermal conductivity measurements using a short transient hot- strip method. Rev. Sci. Instrum. 63 (8); 3966-3971.

Luikov A. V., A. G. Shashkov, L. L. Vasliev, E. Yu Fraiman (1966); Thermal conductivity of porous systems. Int. J. Heat and Mass Transfer. Vol. 11; 117- 140.

Luikov A. V. (1964); *Heat Transfer in capillary porous bodies.* Pergamon Press, Oxford.

Lyall A. (1992); *Materials for building.* Lliffe Books, London Vol. 1.

Mgeladze B. M., G. S. Papava, N. S. Pkhakadze, G. E. Kvantrishvili, N. S. Dokhturishvili and N. A. Maisuradze. (1991); Thermal conductivity of Polymer compositions of Aminoplast. ACTA POLYMERICA. Vol. 42, Iss 2- 3; 89- 91.

Miller M. S. and A. J. Kotlar,(1993); *Techniques for measuring thermal diffusivity /conductivity of small thermal-insulator specimen*. Rev. Sci. Instrum. 64(10); 2954-2960.

Miranda J., A. Oliver, G. Vilaclara, R. Ricomontiel, V. M. Macias, J. L. Ruvalcaba and M. A. Zenteno, (1994); Analysis of Diatomite Sediments from a Paleolake in Central Mexico Using PIXE, X- Ray Tomography and X- Ray Diffraction. Nucl. Instrum. and Methods in Phys. Vol. 85, Iss 1- 4; 886-889.

Mohsenin N. N. (1980); *Thermal conductivity of foods and agricultural materials.* Gordon and Breach; 83-104

Nicolas J., P. H. Andre, J. F. Rivez, V. Debbaut (1993); *Thermal conductivity measurements in soil using an instrument based on the cylindrical probe method.* Rev. Sci. Instrum. 64(3); 774-780.

Odhiambo D. (1969); *Studies in sorption of benzene by Kenya diatomite.* Ph.D. Thesis, London university.

Oswal M. C. (1983); *Text book of Soil Physics.* Vikas Publishing house, PVT Ltd., 1st ed.

Pascoe K. J., Van Nostrand Reinhold. (1978); UK 3 ;391-400.

Revut I. B. and A. A. Rode. (1981); *Experimental methods of studying soil structure* . Amerind New Delhi; 220-236.

Severinghaus N. Jr. (1983), Industrial minerals and rock. 5th ed.; Vol. 1. Am. Inst. of mining, metallurgical and petroleum Engineers, New York, 243- 257.

Singh R., N. S. Saxena, D. R. Chaudhary (1985); Simultaneous measurement of thermal conductivity and thermal diffusivity of some building materials using the transient hot-strip method. J. Phys. D: Appl. Phys. 18; 1-8

Sincich T. (1992); *Statistics by example.* Dellen Pub. Co. 1st ed; 65- 80.

Smith R. C. (1979); *Materials of Construction.* McGrawl Hill UK. 3rd ed.; 25- 40.

Stroud K. A. (1986); *Further Engineering Mathematics.* Macmillan Vol. 2; 30- 85.

Subramanyam S. and C. P. Kothandaraman (1989); *Heat and Mass Transfer-Data Book.* Wiley Eastern Ltd. New Delhi. 4 th ed; 1- 13.

Suleiman B. M. (1994); *Transient Plane Source Technique For Measurement Of Thermal Properties Of Polycrystalline Ceramics Including High-T_c Superconductors.* Department of Physics, Chalmers University of Technology, University of Goteborg; Goteborg, Sweden; 25-60.

Sybil D. P. (1981); *Encyclopedia of Energy.* McGrawl Hill, 2nd ed; 2-38.

Thomas P. D. and C. M. Patton, (1995); *Calculus of Several Variables.* PWS (Thomson), Boston. 1st ed.; 770- 792.

Touloukian Y. S. (1970); *Thermal properties of matter.* TPRC Data series Vol. 1, IFI; Plenum, New York, 223- 405.

Uehera G. and G. Gillman, (1981); *The mineralogy Chemistry and Physics of Tropical Soils with variable charge clays.* Westview Press, Colorado. Ser. 4; 2-40.

Videnov N., S. Shoumkov, Z. Dimitrov, L. Mogilski, L. Brakalov, (1993); Beneficiation of Diatomite Sediments by High Gradient Magnetic Separation. Int. J. Min. processing, Vol. 39, Iss 3- 4; 291- 298.

Woodside W. and J. H. Messmer (1956); *Thermal conductivity of porous media II consolidated rocks.* Can. J. Phys. 34.

APPENDICES

APPENDIX I

Table 14. The adjustments to be made to a mass of sample when it is necessary to increase or decrease its moisture content to a required value (Head, 1989).

	WET SAMPLE	DRY SAMPLE
Initial mass of wet sample	M_1	M_2
Measured moisture content (%)	W1 (>W)	W2(<W)
Required moisture content (%)	W	W
Mass of water to be removed (g)	$(\frac{W_1 - W}{100 + W_1})M_1$	
Mass of water to be added (g)		$(\frac{W - W_2}{100 + W_2})M_2$
Final mass of wet sample required (g)	$M = (\frac{100 + W}{100 + W_1})M_1$	$M = (\frac{100 + W}{100 + W_2})$

APPENDIX II

Correlation coefficient and Least square fit (Sincich, 1992)

Correlation coefficient r is a measure of the linear relationship between two variables, say, V and f(γ), computed as;

$$r = \frac{SS_{vf(\gamma)}}{\sqrt{SS_{vv} SS_{f(\gamma)f(\gamma)}}} \qquad (A.2.1)$$

where, $$SS_{vf(\gamma)} = \sum vf(\gamma) - \frac{\sum v \sum f(\gamma)}{n} \qquad (A.2.2)$$

$$SS_{vv} = \sum v^2 - \frac{(\sum v)^2}{n} \qquad (A.2.3)$$

$$SS_{f(\gamma)f(\gamma)} = \sum (f(\gamma))^2 - \frac{(\sum f(\gamma))^2}{n} \qquad (A.2.4)$$

and n is the number of observations (sample size).

Least square fit procedure

(i) Σv, $\Sigma f(\gamma)$, Σv^2 and $\Sigma v f(\gamma)$ are found from data,

(ii) these values are substituted into the formulae for, $SS_{vf(\gamma)}$ and SS_{vv}

(iii) $\hat{a}_1 = \frac{SS_{vf(\gamma)}}{S}$, and, $\hat{a}_0 = f(\gamma) - \hat{a}_1 v$, (A.2.5)

(iv) Computed values for $\hat{a}_1$ and $\hat{a}_0$ are used to compute the least square fit for $v = \hat{a}_0 + \hat{a}_1 f(\gamma)$. A graph of this equation gives the least square fit.

APPENDIX III

Equation used in calculation of thermal conductivities;

$$V = V_0[1 + Cf(\gamma)] \qquad (A.3.1)$$

$$V_i = V_0 + \frac{V_0^{\,2} I_0 \alpha}{4\pi^{1/2} h\Lambda} f(\gamma_i) \qquad (A.3.2)$$

Where, $I_0 = 0.175$ Amp,

$V_0 = 160.24$ mV $= 0.16024$ V,

$\alpha = 4.4 \times 10^{-3}\ ^{o}C^{-1}$,

$h = 35 \times 10^{-3}$ m.

$C = \frac{V_0^{\,2} I_0 \alpha}{4\pi^{1/2} h\Lambda}$, which is the gradient of equation (A.3.1) above,

therefore, $$\Lambda = \frac{V_0^{\,2} I_0 \alpha}{4\pi^{1/2} hC}. \qquad (A.3.3)$$

For which thermal conductivity is calculated specifically from,

$$\Lambda = \frac{7.96764X10^{-5}}{C} \quad W\ m^{-1}\ K^{-1}. \qquad (A.3.4)$$

APPENDIX IV

Table 15. Value of $f(\gamma)$ for different values of time (t), at constant characteristic times (θ), in the range $0.1 \leq \theta \geq 1.0$

(θ)	0.1	0.2	0.3	0.4	0.5	0.6	0.7	0.8	0.9	1.0
Time (sec)	$f(\gamma_1)$	$f(\gamma_2)$	$f(\gamma_3)$	$f(\gamma_4)$	$f(\gamma_5)$	$f(\gamma_6)$	$f(\gamma_7)$	$f(\gamma_8)$	$f(\gamma_9)$	$f(\gamma_{10})$
10	9.73	6.61	5.20	4.34	3.76	3.32	2.97	2.69	2.46	2.26
20	14.06	9.73	7.78	6.61	5.80	5.20	4.73	4.34	4.03	3.76
30	17.36	12.10	9.73	8.31	7.33	6.61	6.04	5.60	5.20	4.87
40	20.12	14.06	11.36	9.73	8.61	7.78	7.13	6.61	6.17	5.80
50	22.54	15.80	12.78	10.97	9.73	8.81	8.09	7.50	7.02	6.61
60	24.73	17.36	14.06	12.09	10.73	9.73	8.94	8.31	7.78	7.33
70	26.73	18.79	15.24	13.11	11.65	10.57	9.73	9.05	8.48	7.80
80	28.60	20.12	16.33	14.06	12.51	11.36	10.46	9.73	9.12	8.61
90	30.35	21.36	17.36	14.96	13.31	12.09	11.14	10.37	9.73	9.19
100	32.00	22.54	18.32	15.80	14.06	12.78	11.78	10.97	10.30	9.73
110	33.57	23.66	19.24	16.63	14.78	13.44	12.39	11.54	10.84	10.24
120	35.07	24.73	20.12	17.36	15.47	14.06	12.66	12.09	11.36	10.73
130	36.51	25.75	21.00	18.09	16.12	14.66	13.53	12.62	11.85	11.20
140	37.89	26.73	21.76	18.79	16.75	15.24	14.06	13.11	12.32	11.65
150	39.21	27.68	22.54	19.46	17.36	15.80	14.58	13.60	12.78	12.09
160	40.51	28.60	23.29	20.12	17.94	16.33	15.08	14.06	13.22	12.51
170	41.76	29.49	24.02	20.75	18.51	16.85	15.56	14.51	13.65	12.92
180	42.97	30.35	24.73	21.36	19.06	17.36	16.03	15.00	14.06	13.31